Preparation of novel metal-insulin quantum clusters for bio-imaging applications.

A

Dissertation submitted

In partial fulfillment of the requirements for the degree

of Master of Science

In

Biochemistry

Submitted by

Shreya Sharma

(Regd. No.:301607009)

Under the supervision of

Dr. Diptiman Choudhury

Assistant professor

School of chemistry and biochemistry

Thapar Institute Of Engineering And Technology

Patiala, Punjab-147001, India

June 2018

CANDIDATE'S DECLARATION

I, hereby declare that the work being presented in the thesis entitled "Preparation of novel metal -insulin quantum clusters for bio-imaging applications." in partial fulfillment for the requirement for the award of the degree of Master of Science in Biochemistry and being submitted to the School of Chemistry and Biochemistry, Thapar Institute of engineering and technology, is my own work carried out during the period January 2017 to June 2017 under the supervision of Dr. Diptiman Choudhury, Assistant Professor, School of Chemistry and Biochemistry, Thapar Institute of engineering and technology, Patiala. No part of the matter embodied in this thesis has been submitted to any other university or Institute for the award of any degree.

Shreya.

DATE: 22.8.16

Shreya Sharma

PLACE: Patiala

This is to certify that the above statement made by the candidate is correct and true the best of my knowledge.

22/8/16

Dr. Diptiman Choudhury

Assistant professor

School of chemistry and biochemistry

Thapar Institute of chemistry and biochemistry

Patiala -147004

CERTIFICATE

This is to certify that the thesis entitled, "Preparation of novel metal-insulin quantum clusters for bio-imaging applications", which is submitted by Ms Shreya Sharma, in the partial fulfillment for the requirement for the award of the degree of master of science in biochemistry to the school of chemistry and biochemistry, Thapar Institute of engineering and technology, is an authentic record of work carried out by her under our supervision. The contents of this thesis have not been submitted for the award of any other Diploma or Degree.

30/6/18

Dr. Diptiman Choudhury

(Assistant Professor)

School of chemistry and biochemistry

Thapar Institute of engineering and technology

Patiala -147004

ACKNOWLEDGEMENTS

I would like to express my gratitude to my supervisor Dr. Diptiman Choudhury who has an attitude and substance of a genius; he continually and convincingly conveyed a spirit of adventure in regard to research. I'd also like to thank him for the useful comments, remarks and engagement through the learning process of this summer training project. I would like to express my sincere thanks to Dr. Amjad Ali for allowing me to carry out this project in Thapar Institute of engineering and technology, Patiala.

Furthermore I would like to thank Parmandeep kaur (Ph.D Scholar), Pawandeep kaur (Ph.D scholar), Vanshita Goel (Ph.D scholar), Richa Bansal (Ph.D scholar), and Gulshan Kumar (Ph.D scholar) for sticking by my side throughout as well as for supporting me on the way. Without their guidance and persistent help this project would not have been possible.

Also I would like to thank my lab mates who have supported me through thick and thin Aastha Arora, Navpreet Kaur, Sona Bharadwaaj, Aarzoo Sharma, and Riya Gupta who have willingly shared their precious time during this process. I'm highly grateful to my friends Prerna Jain, Alish Vaishnav, Ravinder Kaur and Yash Chandra for supporting me.

I'm highly grateful to my parents for standing by my side like a pillar of strength through little breakdowns and always pushing me further ahead, without their and my grandparent's blessings I wouldn't have completed this project.

Thank you for keeping me harmonious and helping me put pieces together. I'll be forever grateful for your constant support.

THANK YOU ALL AND GOD BLESS!

Shreya Sharma

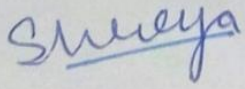

Abstract

This work focuses entirely on a simple and ascendable method for the synthesis of highly fluorescent Au, Cu, Zn, quantum-clusters (QCs) based on colloid synthesis via NaOH mediated synthesis. Exploiting noble metal like Au, and transition metals like Cu, Zn, as model metals. A facile methodology (total synthesis time < 2.5 h) complete with incubation at 37◦C at 240 rpm has been developed to process initially polydisperse, non-fluorescent, and unstable AuQCs, ZnQCs, CuQCs into monodisperse, highly fluorescent, and extremely stable AuQCs, CuQCs, ZnQCs in the same phase (aqueous) and Insulin as protein. The synthetic procedure was successfully stretched to assemble highly fluorescent protected by AuQCs, CuQCs, ZnQCs protected by Insulin, a small peptide hormone consisting of amino acids with functional groups like carboxyl, hydroxyl, and amine etc. The methodology adopted in this study should largely contribute to the practical applications of this new class of fluorescence clusters. In view of the protein protection, coupled with direct synthesis and easy functionalization, this hybrid QC-protein system is expected to have numerous optical and bioimaging applications in the future.

List of abbreviations and symbols

1. QCs – Quantum clusters
2. MQCs – Metal quantum clusters (M= Au, Zn, Cu)
3. iMQCs – Insulin linked metal quantum clusters without incubation
4. IMQCs- Insulin metal quantum clusters with incubation
5. QDs- Quantum dots
6. NCs- nanoclusters
7. MNCs- metal nanoclusters
8. UV-vis – Ultraviolet- visible spectroscopy
9. FTIR – Fourier transform infrared spectroscopy
10. NIR- near infrared region
11. SEM-EDS- scanning electron microscope- Electron dynamic scattering
12. DLS- dynamic light scattering
13. Tyr – Tyrosine (amino acid)
14. Trp – Tryptophan (amino acid)
15. Phe – Phenyl alanine (amino acid)
16. ◦C – Degree Celsius
17. rpm – Rotation per minute

List of figures

List of schemes and tables

Title **Page No.**

Chapter 1

Introduction

The metal quantum-clusters have attracted research interest for their one of a kind part in connecting the "missing gap" amongst nuclear and nanoparticle conduct in respectable metals. Contingent on the quantity of atoms contained in the QCs, when their sizes wind up practically identical to the Fermi wavelength they show optical, electric, charge properties, and tunable fluorescence wavelength (1). It has been found to display sub-atomic like properties, for example, solid fluorescence. These quantum-clusters (QCs), comprising of just a couple to a few many atoms with a size littler than 1-200nm, have risen as an intriguing sort of luminesent nanomaterials.

On drawing a comparison of metal quantum clusters with basic fluorophores, for example, natural colors & semiconductor quantum dabs (QDs), where commercialization can be compelled by nearly poor photostability (for natural fluorophores) or danger concerns (e.g., QDs), fluoresent QCs hence can be viewed as promising substitutes for the plan of creative bio-imaging tests on account of their little sizes because of quantum imprisonment, excellent photostability and lower levels of harmfulness (2). These QCs represent to diverse applications as natural marking, stable chromophores in single-atom microscopy, catalysis, bio-detecting, sub-atomic gadgets, and also optical properties. These QCs have figured out how to attract a feature in an arrangement of highlights that incorporate size, great biocompatibility and amazing photostability, combined with low toxicity levels (3).A distinct feature of the QCs due to their enhanced photostability, large stokes shift, as well as high emission rates are strong luminescence (4).

Luminesense emerges in them because of changes between the dsp inter-band and sp to sp intra-band levels. Subsequently, by moulding the quantity of molecules in the center, outflow wavelength can be tuned effortlessly, fluorescence combined with the non-cytotoxic nature, dissimilar to the prevalent semiconductor QD analogs makes them selective of different biological aplications (5).

Here we report another approach for the union of fluorescent and water-dissolvable Au, Cu, and Zn quantum-clusters utilizing Insulin as the template in aqeuous arrangement (6). Procedure was performed by blending the metal particle antecedent with Insulin and changing it to soluble ph. It is accounted for that fragrant amino acids give electrons to diminish Metal particles (Au, Cu, Zn) while broken disulphide bonds assume real part in balancing out the nucleated bunch.

Utilizing this simple synthesis we can process these polydisperse Hydrocholoauric corrosive (AuCl4), Copper sulfate (CuSO4) and Zinc sulfate (ZnSO4) into stable and to a great degree fluorescent metal quantum-clusters in aqueous medium connected with Insulin as layout (8).

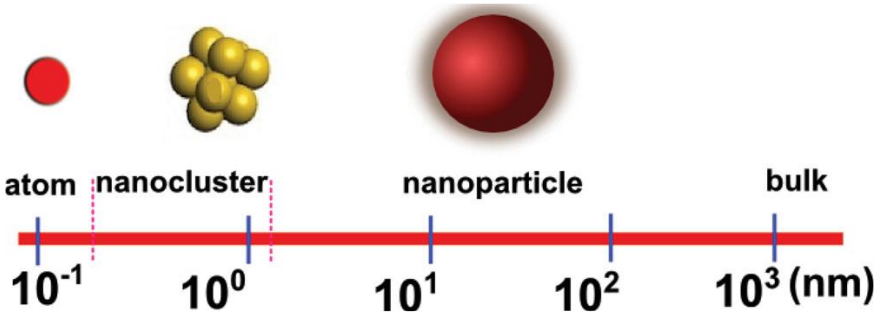

Fig 1: Pyramid of materials from atoms upto bulk particles. The size of metal quantum-clusters fall in-between individual atoms and plasmonic NPs. Reproduced with permission Copyright 2012 [publisher].

Metal	Fermi wavelength (eV)
Au	5.53
Cu	7.00
Zn	9.47

Table 1: Showcases the Fermi wavelength (eV) of the metal atoms that are utilized for fluorescence.

The characterizations of the salt solutions ($AuCl_4$, $CuSO_4$, and $ZnSO_4$), metal salts linked insulin with incubation as well as without incubation were analyzed via exploiting various techniques. It has then summarized the often used techniques for the structural and optical characterizations of copper, gold, and zinc linked insulin quantum clusters such as UV-vis spectroscopy,

Fluorescence spectroscopey, fluorescence microscopy, FTIR measurements, DLS measurements, SEM-EDS analysis.

The most indispensable aspect of this research is Luminescence that is radiated by these metal quantum-clusters (Au, Cu, and Zn). The introduction of insulin as template has unbolted kaleidoscopic dimensions with respect to its functionalities.

Chapter 2

Review of literature

2.1 Nanotechnology: in biomedical sciences

Nano biotechnology has been extensively exploited over the past one decade. It is touted to be the intersection of various fields such as biology, pharmaceutical sciences, biochemistry, biotechnology, chemical engineering etc. the amalgation of these fields has given rise to various dynamic research field areas [10]. This discipline indicates the merger of various biological researches with numerous fields of nanotechnology [11].

This field has led a revolution in the field of biotechnology, by scientists proposing new ideas, recreating and redefining the nano-biotechnology. Many biological systems have been exploited as a motivation for developing new and improved technologies for mankind. Bio-nanotechnology, promises to restructure and refabricate biological mechanisms and pathways in a structured manner by achieving quantum scale level that is beneficial. We can cultivate various bio-mimetic that can provide relief and provision to gain new insights in the biological systems, thereby creating better bio inspired technology [12].

2.2 Fluorescence in image modality

Fluorescence is a molecular phenomenon that is that is unveiled by most organic & non-0rganic substances, centered on the principles of Jablonski diagram. Upon being struck with monochromatic light from another source; the substance under investigation radiates light energy on driving downward to the lower energy level almost instantaneously. The fate of the incident light is that either it is absorbed or reflected, by the substance. In most cases the former phenomena is observed implying that the excuded light is typically of lower energy (& thus

longer wavelength) than that of the source. This process of light captivation and radiation is known as excitation and emission.

Fluorescent molecules can be used directly or atached to other molecules to define the locations of certain structurs within the cell, the presence of certain membrane constituents on the cell exterior (for the identification of cell type), or else used by themselves to substantiate a certain activity within the cell (such as enzyme action) (13).

The utilisation of fluorescense as an imaging modality has become an precious tool for researchers, particularly those in the biological and material science fields, reviewing substances which were hitherto 'invisiblle' under other forms of microscopy (14). In-vivo has opened many gateways for biologists who can improve cell staining techniques by focusing on the specifity and affinity of the fluorophores that can stain specific sub-cellular components, allowing them to highlight their location in the cell and through which we can study potential molecular interactions at very high resolutions (15).

2.3 Quantum clusters: a new dimension in nanotechnology

Clusters can be characterized as agglomerates of a set number of particles or atoms. The quantity of atoms or molecules in a cluster is little in contrast with the quantity of molecules or atoms in a fluid or solid. The average number of closest neighbors of an atom in a cluster does not more often than not compare to its concoction valence (16). Metal quantum groups are developing as gigantic structures for an extensive variety of organic applications because of their small size , tunable optical properties, including optical assimilation, photoluminescense (UV to NIR), non-linear optical properties (2-photon retention, 2-photon fluorescence, & second/third consonant age), ultrafast elements (unwinding energy, electron– phonon coupling, and radiative outflow), and attraction (17). These properties have brought about their utilization in a wide scope of uses, including the detecting of particles (overwhelming metal particles, anions), biomolecules (proteins, DNA, and compounds), natural cells, determination, and treatment (18).

2.3.1 Properties of metal quantum clusters

The properties of bulk metals totally change in contrast with their miniaturized scale counterparts when they're changed to the quantum-measure. Not at all like in the mass, have the quantum-scale metals indicated different colors extending from red to violet, essentially because of the aggregate motions of conduction band electrons, known as surface plasmon reverberation (SPR) (19).

A solitary excitati0n source can quickly prompt the excitation of the QCs with various hues with a vast Stokes move, like semiconductor QDs. This uncommon property permits signal multiflexing for various biotechnological and optical applications. It has been demonstrated that the QCs can display at the simultaneously atom (e.g., super-atom), atoms, & plasmonic nanoparticle (NP) - like properties. The QCs have discrete vitality levels and show atom like assets in the absorption & fluorescence features (20).

2.3.2 Optical properties of metal quantum-clusters

Quantum clusters exhibit greatly enhanced optical properties, this size upshot of electrons present in conduction band can be sculpted on classical electrodynamics prompts them to display optical properties. Due to quantum confinement QCs lose their metallic, ductility properties. This is due to the manifestation of quantized electronic energy levels as compared to their macro-counterparts (21).

Optical properties comprise a crucial role to deliver a unique insight for electric & geometric structures and remarkable evidences for the theoretical calculation. The application of metallic QCs are closely pertinent to their optical properties, such as bio-imaging, photonics, and catalysis (22).

2.3.3 Photoluminescence of metal quantum-clusters

Outsized stokes shift and good photostability are the distinct features that are responsible for photoluminescence of metal QCs. It has been difficult to trace the foundation of photoluminescence in metal QCs (23). Nevertheless, there are some aspects that have been known to dominate their influence on photoluminescence of QCs, counting the electron energy quantization effect, metal–ligand interaction, & metal core charge state, as well as the surface effect. Through dwindling size from NP to QC, the ensuing discrete electronic structure in QCs is moderately accountable for the fluorescence properties (24).

Among the various testified metal QCs such as Au, Ag, Cu, Pt, Pd NCs, Au and Ag QCs are furthermost prevalent, mainly because of their astonishing stability, strong fluorescence, noble bio-compatibility, and tunable emission in the visible to NIR spectral region (25).

2.3.4 Protein linked metal quantum-clusters

0wing to its biological importance insulin has attracted a great covenant of scientific exploration during this century. Nobel Prize was awarded in 1958, to Fred Sanger from Cambridge University for executing task of sequencing the amino acids of insulin (26).

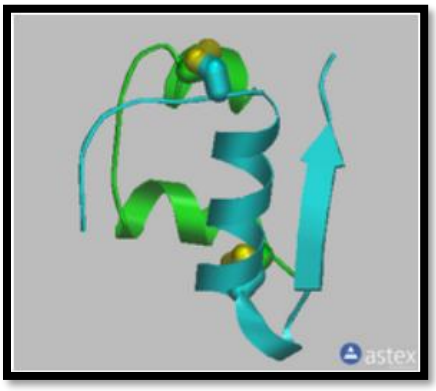

Fig 2: Proinsulin is transformed to insulin. Proinsulin is shown, highlighting the A chain (green), & the B chain (cyan) and the C-peptide is expunged to vintage mature insulin. The two intermolecular disulfide bonds have been demonstrated (26).

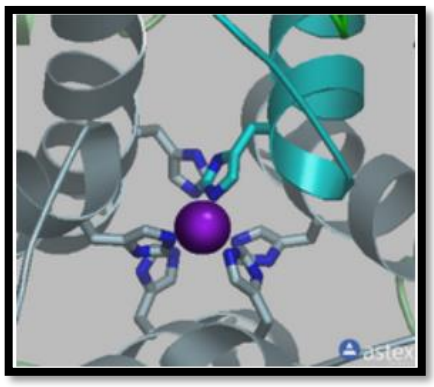

Fig 3: Insulin forms a hexamer. A monomer, consisting of an A chain (green) and B chain (cyan), forming a dimer with another monomer. Three dimers then compile and form a hexamer. Two zinc ions on the central threefold axis (purple

spheres) are coordinated by His residues (shown as sticks) (26).

Insulin stands created in the β cells of the islets of Langerhans present in the pancreas. At first, chemicals expel the N-terminal flag succession from pre-proinsulin (a bigger unfurled peptide chain) to give pro-insulin (an antecedent, single-chain idle shape). The interfacing C-peptide is then expelled from pro-insulin via chemical to give insulin. Insulin is put away in the pancreas as hexamers, prepared to be discharged because of outside jolts. Insulin is shaped from two chains of amino acids connected together synthetically by disulphide spans framed between the side-chains of four of these amino acids (27).The A chain encompasses 21 amino acids and the B chain 30. The two chains crease together to frame the smaller, 3-D insulin at0ms. The requirement for this nitty gritty information of insulin's 3-D structure that has made it likely for specialists to discover methods for changing its properties (28). New insulin arrangements emerges from the need to emulate all the more intently, in individuals with diabetes the typical physiological plasma insulin profile, however additionally limiting their uneasiness and unconvienience (29). Metal NCs are little and in this manner the ordinary organic elements of these biomolecules may not be aggravated or if nothing else negligibly exasperates. Because of every one of these focal points, bio-related uses of metal NCs have pulled in awesome enthusiasm for late years (30).

2.3.5 Protein linked metal quantum-clusters imaging

Albeit organic dyes with splendid fluorescence has been generally utilized as fluorescence indicators for a long time, their deficiencies, for example, constrained photo-stability and little Stokes shift may hold back their long haul utilization in tracking or multicolor imaging applications. Semiconductor QDs possess brilliant shine and photostability; in any case, measurements of numerous quantum dots are regularly over 5 nm, which may cause main active or steric obstruction issues for contemplating biomolecule collaborations or following natural procedures. Fluorescent metal QCs have been shown as helpful tests for bio-imaging (31).

Their favorable circumstances, for example, ultrasmall measure, great photostability, low cytotoxicity, great bio-compatibility, substantial Stokes shift, high emanation rates, and close infrared (NIR) discharge makes metal QCs as appealing fluorescent tests for bio-imaging. Among different metal QCs, fluorescent Au and AgQCs have been for the most part sought after for bio-imaging application in view of their high solidness and very much created union strategies (32).

2.4 Three major synthesis methods of cluster formation

2.4.1 Inverse Micelle synthesis

The key part of this technique which extricates it from either fluid or gas atomic conglomeration process forms is that metal group development is meticulous by the small scale heterogeneous condition of the bead like backwards micelles. An extra preferred standpoint is the reasonable, prepared accessibility of simple salts as atom sources for the development procedure. Most metal organic sources of metals do not decompose at regulated temperature for fluid phase synthesis and are harmful and costly.

In many liquid phase formation procedure combination conventions, regulation of the final cluster size can be managed:

- By the centralization of metal salt precursors.
- The micelle volume generally decides the maximum size of the atomic clusters which may trade amid the development or collection advance of the amalgamation.

The most critical change is the expansion of emphatically restricting surfactants, for example, thiols or amines to the opposite micelles arrangement encompassing the disintegrated metal salts (33).

2.4.2 Cluster development in polar organics via chemical reduction

Cluster formation in polar organics by compound decrease within the sight of stabilizers initially detailed by Hirai et al. This strategy for metal cluster development uses substance decrease of a orgranic soluble metal-salt precursor. Moreover a co-coordinating or non- coordinating solvent

can be utilized, or some blend thereof. He likewise researched together the synergist action and the development instrument of the metal NPs ensured by the polymers poly (vinyl liquor) or poly (N-vinyl-2-pyrrolidone) (PVP). They set up an engineered technique to frame PVP-secured Pd NPs by the without water decrease of Pd acetic acid derivation utilizing a liquor.

The benefit of this strategy is that ligands in the metal natural complex could be decreased and removed from the nanocrystal surface and consequently were more averse to taint the group surface. In all the arrangement techniques for change and base metal bunches the general rule of the utilization of littler measures of settling ligand and bigger antecedent metal salt fixations to shape bigger groups is substantial (33).

2.4.3 Organometallic decomposition in the presence of stabilizers

Decay of a thermally labile, oil solvent, metal-natural forerunner is the most established approach for non-fluid combination of metal quantum-groups. This approach requires the nearness of a surfactant-like stabilizer, for example, a square co-polymer. Decently monodisperse colloids can come about under the best possible conditions. This strategy is ordinarily utilized for base-metal quantum-group union like Co, Fe, Ni since an accessible thermally flimsy metallo-natural is required, for example, $Fe_3(CO_5$, $Co_2(CO)_8$, $Ni(CO)_4$. These mixes are exceptionally air-delicate and either somewhat or seriously poisonous. It is therefore critical that all dealing with be d0ne in either a glove box, or by Schlenk-line techniques. Because of the fast development rate contrasted with substance lessening techniques, the last bunches are typically exceptionally defective and require critical strengthening at raised temperatures to deliver fantastic examples. In this strategy the quantum-bunch estimate is expanded by expanding the measure of antecedent and additionally diminishing the measure of surfactant. With a specific end goal to accomplish an ideal combination utilizing this strategy, some experimental variety of temperature and lessening operator is vital. This is on account of a portion of the solvents may not permit solubilization of all the accessible parts (33).

2.5 Other methods of cluster synthesis

2.5.1 Electrostatically reduced phase electron transfer

There are two principle techniques for planning fluoresent metal NCs. The primary methodology is the template assisted synthesis. Here biomolecules (e.g., proteins & DNA), dendrimers (e.g.,

poly (amido amine) (PAMAM)) & polymers (e.g., poly (methacrylic corrosive) (PMAA)) are utilized as a layout to direct the development of fluorescent Au or potentially Ag NCs. Be that as it may, the as-blended metal NCs are installed in the layout particles, prompting a generally huge hydrodynamic width (>3 nm), which may influence their ease of use as a fluoresccent name for little atoms or few-nanometer-sized biomolecules.

The second tactic depends on the utilization of particular capping agents, e.g., thiol ligands, which associate strongly with the noble metal surface to shape ultra-fine-sized metal NCs ensured by a monolayer of thiol ligands (34).

2.5.2 One pot green synthesis

Encouraged by the work of Shao et al., herein, a one-pot green process is used to synthesize noble metal clusters (Au and Pt) with diverse luminescence by utilizing chicken egg white as templates at room temperature in aqueous solution. Chicken egg white that is in fact used as raw material is cheap; no extra energy consumption is required like no stirring. It is easily operated at room temperature with mild reaction conditions. N0 organic solvents, hazardous agents are utilized. The synthesis reaction is carried out by mixing the two solutions, and very strong luminescence is observed (35).

2.5.3 Colloidal method in aqueous phase

The chemical reduction of a suitably picked metal precursor salt in a fluid state. These wine-red sols showed momentous steadiness because of charge adjustment by means of adsorbed citrate particles. This steadiness is shown by the way that examplse arranged in fixed vials by Faraday in the mid-1850s can even now be seen in the Cavendish historical center in Cambridge. Be that as it may, this general technique, even with its cutting edge refinements isn't effectively stretched out to other comparable metals like Ag or Pt. Nor can an extensive variety of sizes with tight polydispersity or high fixation be effectively created (34).

2.5.4. Colloidal method in Non aqueous phase

Researchers have just as of lately created non-aqueous techniques for colloidal combination using steric, rather than charge, adjustment. Ligands, ordinarily surfactants or

amphiphillic polymers are available amid the cluster development and avert collection between groups by keeping the group surfaces separated amid crashes in arrangement. An early case of this approach which eventually prompted the advancement of attractive particles for recording designs was that of Hoon et al. They created Co colloids (now called nanoclusters, nanocrystals, or nanoparticles) in the 1– 100 nm run by thermolysis of $Co_2(CO)_8$ within the sight of dispersant polymers (34).

2.5.5. Monodisperse method

The superlative examples of monodisperse metal cluster development from atomic precursors in solution were put forward by Schmid. This work demonstrated that the part of the ligand is to sterically stabilize out inorganic quantum-clusters in a solvent and it was basic in deciding the eventual structure and staple size of a given quantum-cluster.

Given the constraints laid out above for organometallic routes to metal groups, a more general quantum-cluster combination which consolidates the benefits of low harmfulness/cost antecedents, and high return of conventional fluid centered colloidal science with the size scattering control and concoction adaptability of organometallic strategies would be very helpful.

Because of this objective Boutonnet, Kizling, and Stenius first utilized aqueous pools of water found in oil-persistent micro-emulsions to solubilize basic ionic metal salts of Au, Pd, Pt, and Rh, trailed by synthetic diminishment utilizing hydrazine or hydrogen gas to create metal clusters scattered in oils. Such new nanomaterial was later appeared to have great synergist movement for hydrogenation (34).

2.6 Applications of protein linked quantum- clusters

2.6.1 Biological imaging: Cell imaging in-vitro

Dickson et al. have completed a ton of researches concentrating on the cell imaging in view of the AgNCs. In 2007, Dickson et al. built up the peptide-ensured fluorescent AgNCs for effective cell imaging. In situ silver-stainad cells unequivocally upheld the perception of fluorescent AgNCs in cells, showing that nucleolin and other argyophilic proteins might be exceptionally helpful aides for biocompatible AgNC planning (36). When contrasted with AgNCs, AuNCs might be more appropriate for cell-imaging in light of their extraordinary close infrared glow properties and magnificent colloidal sound qualities (37). Because of the great bio-compatibility and photo-stability of AuNCs, such incorporated AuNCs were likewise used for the optical imaging of live HeLa cells utilizing confocal microscopy. AuNCs an intense test to recognize growth cells from typical cells. CuNCs, as one sort of recently rising metal nan0cluster, can likewise be connected for cell imaging. A bifunctionall peptide was intended to in-situ diminish Cu particles and stay a CuNCs. The peptide– CuNCs test, essentially made out of Cu14, transmitted blue two photon fluorescence under femto second laser excitation. The test was likewise appropriate for one-photon and two-photon cell cores imaging for both HeLa and A549 cell lines (38).

2.6.2 Bio-imaging *in-vivo*

In vivo imaging is an intense method for confinement and dynamic observing of biomolecules in living frameworks. The improvement of novel in-vivo imaging sensors would give huge progresses toward clinical and medicinal diagnostics. Gold quantum-clusters with the infrared (NIR) fluorescence are invaluable to be utilized *in vivo* imaging because of profound tissue entrance, least photo harm to organic examples, and least obstruction from foundation auto fluorescence by biomolecules in living frameworks. Zheng et al. has played out a genuine work in bio-imaging in vivo by using AuNCs (39). In 2011, they found that the luminescent GSH–AuNCs showed the effective renal clearance. This new finding came about because of the plain little molecule estimate and the GSH ligand, which not just empowered most of the luminescent AuNCs to be removed from the body via kidney filtration, yet in addition settled the luminescent AuNCs amid blood disemination. Motivated by these advances, it could be profoundly encouraging to be connected for in-vivo bio-medical imaging. Zheng et al. likewise found that GSH– AuNCs with breadths of B2.5 nm acted like little color atoms (IRDye 800CW) with great physiological solidness, effective renal leeway yet an any longer tumor maintenance time and speedier ordinary tissue freedom (40).

2.6.3 Metal quantum clusters in image-guided cancer therapy

Optical imaging-guided malignancy treatment is a promising innovation for concurrent tumor imaging and treatment. Due to the superb optical properties, metal quantum clusters may have incredible potential for applications in imaging-guided malignancy treatments (41).

In 2011, Irudayaraj and colleagues announced BSA-ensured AuNCs, which were conjugated with herceptin, for particular focusing on and atomic restriction in ErbB2 over-communicating bosom growth cells and tumor tissue (42).

2.6.4 Sensing

Numerous groups have worked together on metal ion sensing such as Hg^{2+} (43), Cu^{2+} and Pb^{2+} using QCs linked to protein; their facile synthesis types them as commercial tools for such applications. Demonstrated by Xie et al, that AuQC of BSA can be utilized as a sensor for Hg^{2+}. Similar applications were proposed by Wei et al. and Lin et al. who synthesized AuQCs in lysozyme and had revealed its Hg^{2+} sensing claim. In general, it is reported that Hg^{2+}quenches fluorescense by interacting with the core while on the other hand fluorescence quenches due to the aggregation caused by Cu^{2+} ions. AuQC in NLf was testified to be sensitive to Cu^{2+} ions other than Hg^{2+}. AuQCs in BSA developed by Muhammed et al. also displayed metal enhanced fluorescence, fluorescence was not witnessed in the presense of $Cu^{2+}$and was visible in the presence of glutathione. Various other proteins containing $AuQCs_s$ and $AgQCs_s$ have been engaged for metal ion sensing sach as trypsin, pepsin, ESM. Also AuQCs in horseradish peroxidase has been exploited to detect H_2O_2 (44). Wang et al. and Liu et al used AuQCs in BSA for the recognition of glutaraldehyde in water and for the detection of cyanide respectively (45). Recently Goswami et al. synthesised blue emiting CuQCs in BSA and revealed that it can be utilised as a sensor for H_2O_2 and Pb^2 (46).

2.6.6 ECL based sensing

Aside from coordinate metal particle detecting, Electro-chemical-Luminiscense (ECL) based detecting has likewise been illustrated. Li et al. shown that ITO covered AuQCs in BSA displayed ECL and detailed that ITO assumed a noteworthy part in upgrading ECL. They detailed that within the sight of anionic co-reactant $S_2O_8^{2-}$ (47). ECL was improved and exhibited its application to identify dopamine. Tooth et al. demonstrated the age of ECL via AuQCs in BSA within the sight of tetraethyl amine (TEA) and demonstrated that ECL is distinctively

impacted by metal particles; here they indicated it to be influenced by Pb^{2+} (48). As of late, graphene conjugated AuQCs in BSA has likewise been utilized for producing ECL Hun et al. as of late utilized AuQCs in BSA in chemiluminescense based tests for the recognition of lysozyme in cell (49). Anti-bacterial fusions have likewise been made utilizing NMQCs in proteins. Chen et al. revealed that AuQCs in lysozyme has improved antibacterial action against safe strain (47).

2.6.7 Several other applications of metal linked protein quantum clusters

A few organic utilizations of the NMQCs in proteins have likewise been illustrated. Retnakumari et al. demonstrated that AuQCs in BSA conjugated with folic corrosive can be viably used to focus on the folate receptors in disease cells; this was the principal answer to utilize QC in protein for atomic receptor particular application and in another report, they indicated AuQCs in BSA can be conjugated to monoclonal antibodies and utilized for focused discovery of intense myeloid leukemia cells (50). Likewise, Muhammed et al. have additionally indicated folate receptor particular take-up of AuQC in BSA by human epidermoid carcinoma KB cells. As of lately, Wang et al. have conjvgated AuQCs in BSA to herceptin (a broadly utilized adapted monoclonal immunizer if there should arise an occurrence of bosom disease) to atomic target Erb2 over-communicating HER 2+ bosom tumor cells for focused growth treatment (51). Unconjugated AuQCs in BSA were not taken up by cells, along these lines exhibited the focusing on capacity. Beforehand, to give usefulness of one need to depend on conjugation science to conjugate with bio-functional atoms, now because of the landing of QCs in practical proteins, bio-usefulness ends up characteristic. AuQCs in insulin has been utilized for bio-imaging of mind cells and as a CT differentiate operator (52). Industrially accessible insulin and AuQCs in insulin are appeared to diminish the blood level glucose in a comparative way and no significant change was watched. They proposed that the safeguarding of bioactivity of insulin, even after the arrangement of groups in them, is principally due to the flawless disulphide bonds. They additionally have demonstrated that in indistinguishable myoblast cells having less number of insulin receptors, take-up of AuQCs in insulin was less contrasted with the separated myoblast cells having expanded number of receptors (53).

Table 1

List of proteins used for NMQCs synthesis and their demonstrated applications

Protein	Metal cluster	Study and application
Bovine serum albumin	Au, Ag, Cu	Sensing of Hg^{2+}, Cu^{2+}, Pb^{2+}, H_2O_2, Glutaraldehyde, and cyanide, electrochemiluminescence, cluster evolution, bio-imaging and *in vivo* imaging.
Lysozyme	Au	Hg^{2+} sensing, antibacterial activity
Cellular retinoic acid binding protein II	Au	
Lactotransferrin	Au	Cu^{2+} sensing, FRET, composite with graphene cluster evolution and bio imaging
Insulin	Au	Grown in crystals, bio imaging and bioactivity
Pepsin	Au	Hg^{2+} sensing, Blue, green and red emitting Au_{QC}
Trypsin		Hg^{2+} sensing
Serum transferrin	Au	Bio imaging
Egg shell membrane (mixture of proteins)	Au, Ag	Hg^{2+} sensing
α-Chymotrypsin	Ag	Cluster-protein interaction
Horseradish peroxidase	Au	H_2O_2 sensing
Human serum albumin	Au	NOx sensing

Table 2: Showcases applications of various NMQCs linked with proteins

Chapter 3

Materials and methods

3.1 Objective

The objective is twofold:

1. To synthesize insulin capped metal quantum-clusters.
2. To perform bio-imaging on Lung cancer cells (A549).

3.2 Materials and methods

All the glassware was washed with acid followed by water and later dried, prior to use.

All the solution was prepared using MilliQ water. All the materials required were autoclaved prior to their usage

Insulin (Elli lilly 70/30 human insulin), Lung cancer cell line(A549) Glass vials, Aluminum foil paper, magnetic stirrer REMI 2MLH, magnetic beads, oven, NaOH solution (Avantor performance Materials India limited, Gujarat India), $HAuCl_{4.3}H_2O$ (Hyaluronic acid), $CuSO_4.5H_2O$ (Copper sulphate pentahydrate), $ZnSO_4$ (Zinc sulphate) solution, HCl (0.1 N Hydrochloric acid), 2% Formaldehyde solution, PBS buffer, 6 well plate, pipettes, Fluorescence microscope, incubator, p^H Paper. All solutions were purchased from LOBA chemicals.

The insulin linked metal nanoclusters were synthesized and were utilized to showcase fluorescence in Lung cancer cell line (A549).

3.3 Preparation of insulin linked metal nanoclusters

Standard protocol was followed for all the three mentioned salts 3.47 M fresh insulin was taken and was converted to 1.486mM. In which 536ul of insulin was added in a covered glass vial and to this NaOH solution was added to adjust the p^H to 10.5 (SOLUTION A). The salt solutions of

1.82mM ($AuCl_4$, $CuSO_4$, and $ZnSO_4$) were prepared in a covered glass vial (SOLUTION B). Now these two solutions were mixed and the p^H was adjusted to physiological p^H 7.4 using HCl (0.1N). The resulting solution was kept for incubation for 48 hours at 37◦C at 240 rpm.

3.4 Addition of MQCs - insulin in the lung cancer cell line (A549)

The samples were incubated in the UV light in UV- laminar air flow for 1 hour. Then 10µl of each sample i.e. the metal salts ($AuCl_4$,, $CuSO_4$, and $ZnSO_4$) linked with insulin quantum clusters were added to the lung cancer cell line. The sample was given washing PBS buffer twice to remove any kind of impurities. Later 2% formaldehyde solution was added to fix the cells. The cell lines with the added samples were kept for incubation for 2.5 hr and later the cover slip was transferred onto the glass slides and the images were observed using fluorescence microscope.

3.5 Characterizations

3.5.1 UV- visible spectroscopy (UV-2600 spectrophotometer Shimadzu)

After synthesis of Insulin linked metal quantum clusters ($AuCl_4$, $CuSO_4$, $ZnSO_4$), UV-visible absorbance was measured using (UV-2600 spectrophotometer shimadzu) and 4000µl quartz cuvette with 1cm path length, it was operated from 200nm to 1100nm.Measurements were observed for salt solutions ($AuCl_4$, $CuSO_4$, $ZnSO_4$), Insulin metal quantum clusters with incubation and insulin metal quantum clusters without incubation were measured to study the interactions between Insulin and metal quantum clusters.

3.5.2 DLS measurements

DLS measurements were conceded out to determine the hydrodynamic size of the sample post their washing to remove any kind of impurities. The samples (IAuQCs, IZnQCs, and ICuQCs) after preparation were handed over for DLS measurements.

3.5.3 Fluorescence spectroscopy (Agilent technologies Cary eclipse)

Agilent technologies Cary eclipse fluorescence spectrophotometer was exploited to determine the binding of insulin to the metal quantum lusters using the three mentioned samples. The fluorescence intensity was measured at an excitation wavelength of 302 nm and 365 nm, coupled with an emission scan from 300 nm to 800 nm with excitation and emission slit of 10mm.

3.5.4 FTIR Analysis (Agilent Cary 600 series FTIR Spectrophotometer)

Agilent Cary 600 series FTIR Spectrophotometer was exploited for analyzing the functional groups of the three mentioned samples. The samples were washed prior to use to remove any kind of impurities. The samples were air dried onto a glass slide at 37◦C. The pellets were formed by mixing the samples with Pottasium bromide (KBr). The scan was observed from $4000cm^{-1}$ to $400cm^{-1}$.

3.5.5 Fluorescence microscope (Dewinter)

The fluorescence of the samples was determined by Dewinter fluorescence microscope, for the samples as mentioned above. The intensity was measured by incubating the samples for 1 hour in UV light to remove any kind of impurities. After that 10µl of each sample was poured in, to check the fluorescence of the sample on A549 (Lung cancer cell line). Then the microscope was adjusted to check fluorescence at various wavelengths.

3.5.6 SEM-EDS (SEM JEOL JSM-6300)

Scanning electron microscope – Electron dynamic scattering was performed to analyze the percentage of different elements present in the samples. It was performed by centrifuging the samples at 240 rpm for 10-15 minutes, later the pellet was thoroughly washed in order to remove any kind of impurities or unbound metal salt associated with the samples (IAuQCs, IZnQCs, and ICuQCs). The pellet was investigated to analyze the elemental constituents in the samples. To characterize the bound quantity of metal (Au, Zn and Cu) present in the sample linked with insulin.

Chapter 4

Results and discussions:

4.1 Absorbance spectra

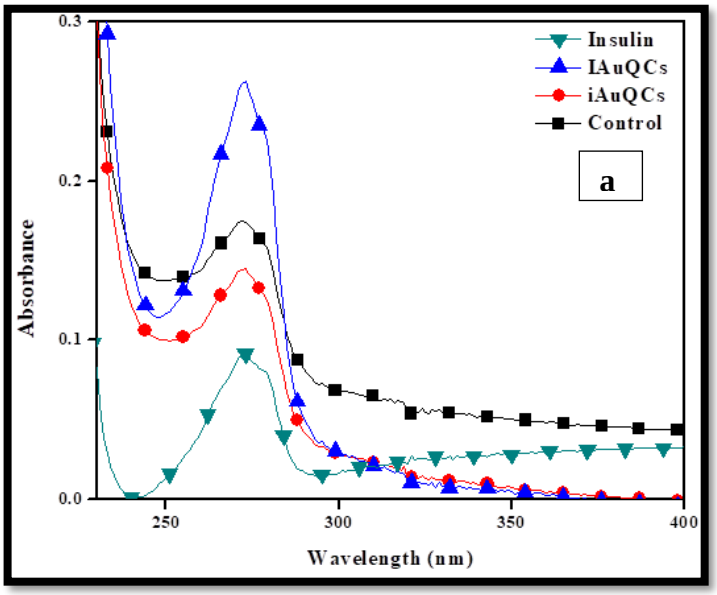

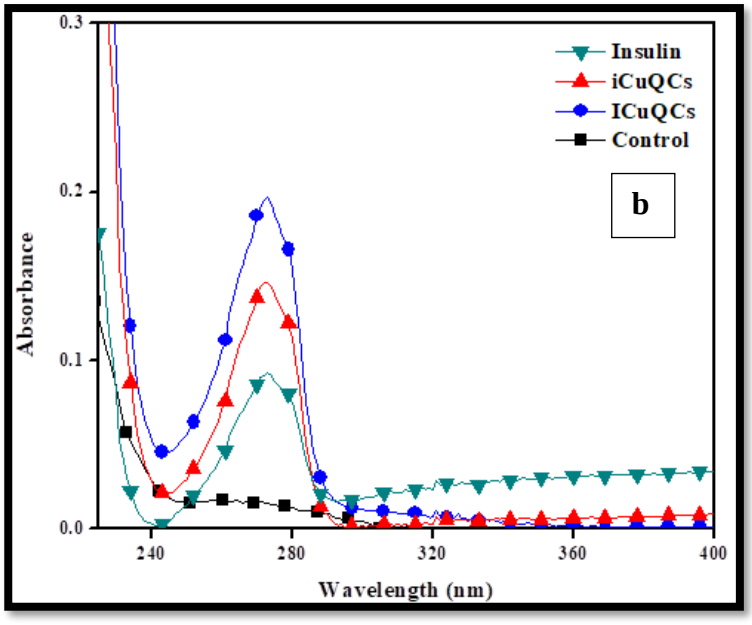

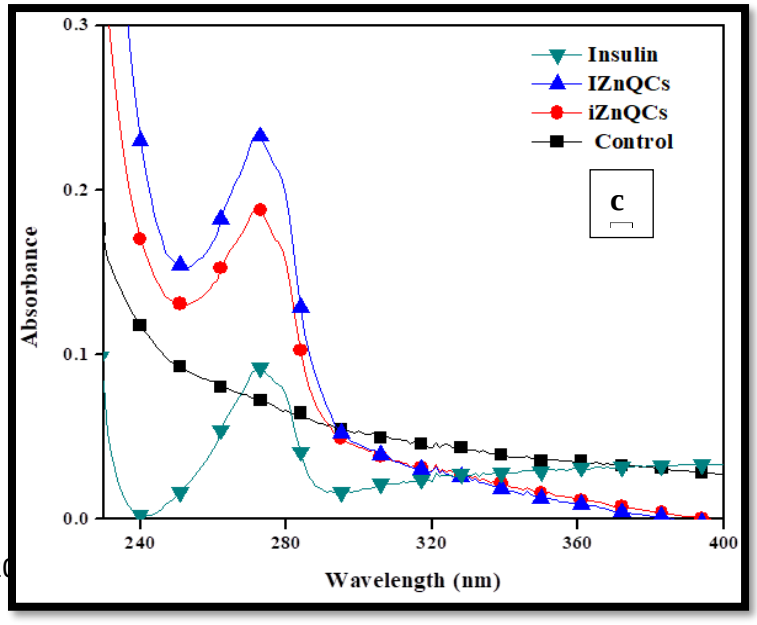

Fig 4: UV-vis spectroscopy of all the three samples (in anticlockwise fashion) i.e. metal salt solutions, iMQCs, IMQCs, and insulin. (Where M= Au (a), Cu (b) and Zn(c)).

Insulin encompasses four Tyr and three Phe residues. In the absenteeism of Trp, Tyr dictates the absorption spectrum of proteins to the exclusion of Phe and non-aromatic absorption attributable to cystine, histidine, or the peptide bond. It has been establish that protein denaturation results in evident consistency in its fluorescence characteristics, and that is what was expected for insulin under the experimental conditions used in this study. A sigmoid is observed in Tyr fluorescence during insulin aggregation. The three native disulphide bonds present in insulin are responsible for the quenching of the partial hydrophobic bonds of Tyr .The interactions that occur between Tyr residues & disulfide bonds can only occur upon contact of hydrophobic clusters to the solvent. As this hydrophobic bond is exposed the peak sharpens due to formation of the desired clusters.

IAuQCs displayed a sharp absorption peak with maximum at 272 nm at a relatively higher absorbance. This is indicative of the fact that $AuCl_4$ has been reduced by the disulphide bonds of Insulin leading to the formation of quantum clusters. The iAuQCs exhibited a comparatively broader absorption peak at 271nm with lower absorbance. Thus the sharpness of peak confirms the formation of quantum clusters.

Similar behavior has been observed in transition metal (Zn and Cu) capped insulin quantum clusters. For ICuQCs showcased an absorption peak with maximum at 273.2 nm, with a sharp peak and higher absorbance. On the contrary the iCuQCs acquired a peak with maximum at 272.5 nm, coupled with lower absorbance. The peak however was broader in comparison to the former sample.

IZnQCs depicted a sharper peak in the absorption spectra with maximum at 272.71 nm. While on the other hand iZnQCs showcased a broader peak with maximum at 272.75 nm.

Only insulin solution that is the same for all the three samples showcased an even broader peak also at 272nm, which could be accredited due to the presence of amino acids in proteins, particularly Tyr which is responsible for fluorescence of insulin. As it gets exposed the fluorescence intensity increases and is responsible for cluster formation.

4.2 DLS measurements:

The DLS analysis is indicative of the hydrodynamic size of the samples i.e. $AuCl_4$, $CuSO_4$, $ZnSO_4$ linked with insulin.

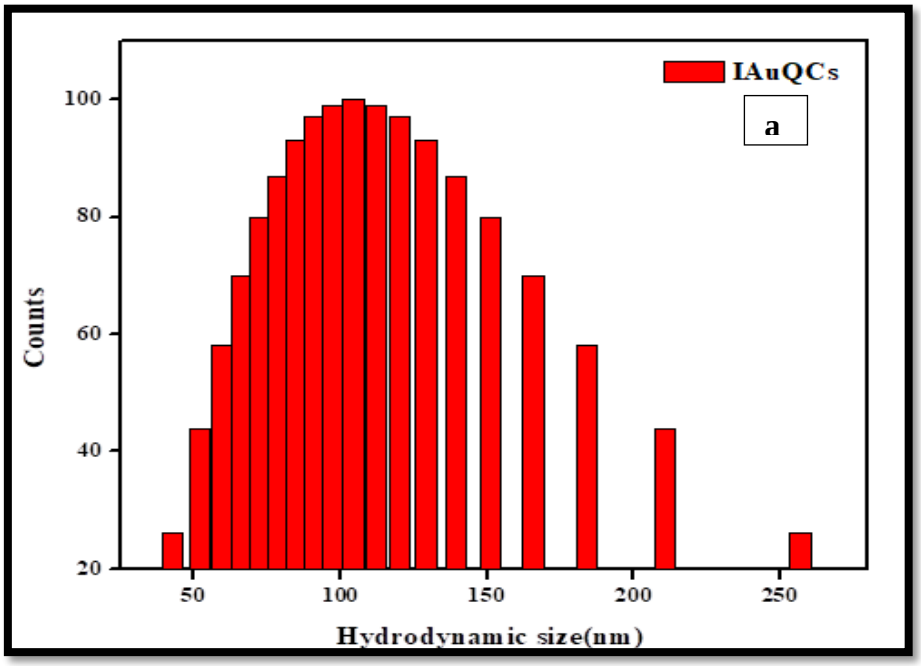

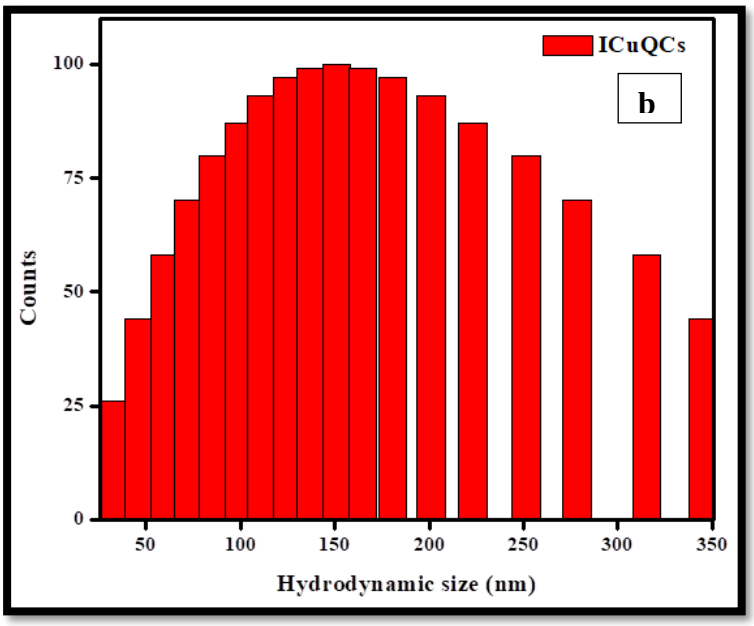

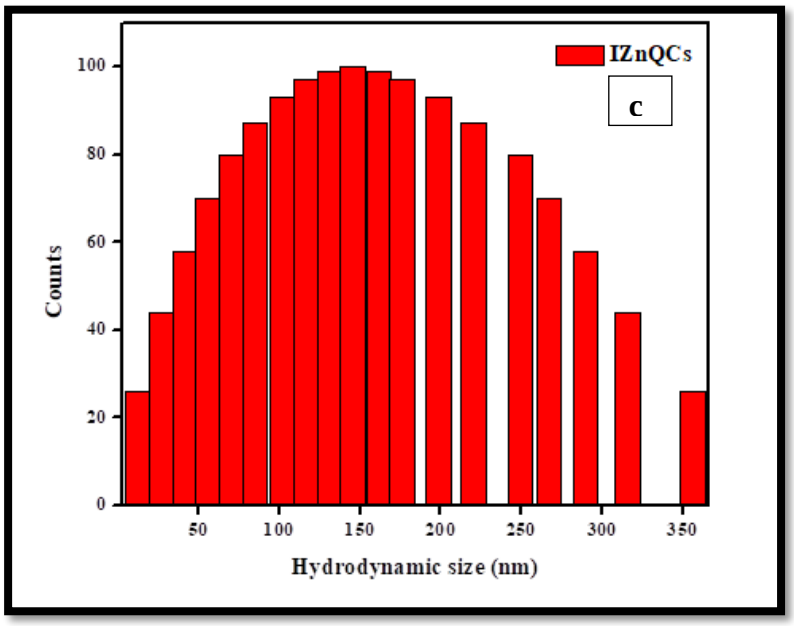

Fig 5: The graphs DLS of IAuQCs (a), ICuQCs (b), and IZnQCs (c).

SAMPLES	HYDRODYNAMIC SIZE (nm)
IAuQCs (a)	60.0 nm
ICuQCs (b)	153.4nm
IZnQCs (c)	146.5 nm

Table 3: The above table showcases the hydrodynamic size (nm) of the different samples.

4.3 FTIR spectra

FTIR measurements of salt solutions (**$AuCl_4$**, **$CuSO_4$**, **$ZnSO_4$**), salt solutions with insulin capped (incubated) and only insulin solution were carried out.

The FTIR graphs were plotted in two comparisons:

4.3.1 The incubated samples capped with insulin in comparison with insulin solution.

Here for only Insulin solution and ICuQCs shows a peak at 653 nm which depicts aliphatic C-C stretch, while for IZnQCs and IAuQCs depicts a peak at 684 nm which implies a shift in peak. The aromatic C=O stretch is observed to be similar for insulin and ICuQCs at 936 nm, 988 nm, on the other hand for IZnQCs shows only a one peak at 988 nm and IAuQCs shows one peak at 915.7nm. The amine C-N stretch is observed to be similar for all Insulin solution, for IZnQCs and ICuQCs shows a peak at 1093 nm while IAuQCs, 1124nm which shows a peak difference. The peak of Aromatic C-C stretch for Insulin only, ICuQCs and IZnQCs shows a peak at 1428.6nm whereas 2 peaks for IAuQCs, 1397 nm and 1428.6 nm. Aromatic C=C bend shows different peaks for only insulin solution it shows peak at 1533 nm , for CuSO4 linked with insulin the peak is present at 1553 nm, for ZnSO4 linked with Insulin the peak is displayed at 1586 nm but it is absent for IAuQCs. Now the amide C=O stretch bond appears at 1659.4 for Insulin solution, ICuQCs and IZnQCs but for IAuQCs the peak appears at 1649 nm. The nitrile stretch for insulin solution and ICuQCs shows the peak 2372.5 nm, whereas the 2 peak appear for IZnQCs, 2319.7 nm, 2372.5 nm, for IAuQCs shows a peak at 2372 nm. The O-H stretch

appears at 2917.7 nm for insulin solution and for ICuQCs but for IZnQCs two peaks appears at 2864.9 nm and 2917.7 nm, whereas for IAuQCs 2949 nm. Amine stretch appears at 3389.7 nm for insulin solution, ICuQCs and IZnQCs, whereas for IAuQCs appears at 3410 nm.

4.3.2 The incubated samples capped with insulin in comparison with their corresponding salt solutions

S-S stretch is absent for CuSO4, ZnSO4 and AuCl4 solutions but shows a peak at 588.4nm the peak appears at ICuQCs, IZnQCs, and IAuQCs. The aromatic C-H stretch is same for $CuSO_4$ solution and ICuQCs; $ZnSO_4$ solution and IZnQCs i.e. 610 and 610.7 nm respectively. The aromatic C=S bend was observed only in metal salts linked with insulin but were absent for only metal solutions, for ICuQCs showed a peak at 854nm, for IZnQCs 762nm, for IAuQCs showed a peak at 861.7nm.The C=O stretch appears at ICuQCs 917.4nm, for ZnSO4 peak appears at 988nm, and for IAuQCs the peak appears at 966nm. ICuQCs and IAuQCs show the amine C-N stretch peak at 1093 and 1055nm respectively, whereas two peaks for $ZnSO_4$ solution and IZnQCs at 1094nm. Aromatic C=C bend peak appears for ICuQCs, IZnQCs and IAuQCs at 1533nm, 1586nm, 1659nm. Amide C=O stretch is same for ICuQCs and IZnQCs linked with insulin at 1642nm, IAuQCs shows a peak at 1689nm. The nitrile stretch is similar for all $CuSO_4$ and $ZnSO_4$ solution, ICuQCs and IZnQCs the peak appears at 2372nm, whereas the peak for IAuQCs appears at 2348nm. A broad O-H band is observed at 2994nm for ICuQCs, for IZnQCs the band appears at 3065nm, for IAuQCs the peak appears at 2912nm. The amine stretch is observed only for IZnQCs at 3516nm, for IAuQCs the peak appears at 3462nm.

The FTIR data of insulin and the samples is perfectly aligned, which is suggestive of the fact that the peaks observed in only insulin solution are also observed in the IMQCs (where M= Au, Cu, and Zn). The peaks in the salt solutions do not correspond to the peaks in the IMQCs. Hence we can say that the insulin linked metal clusters are formed.

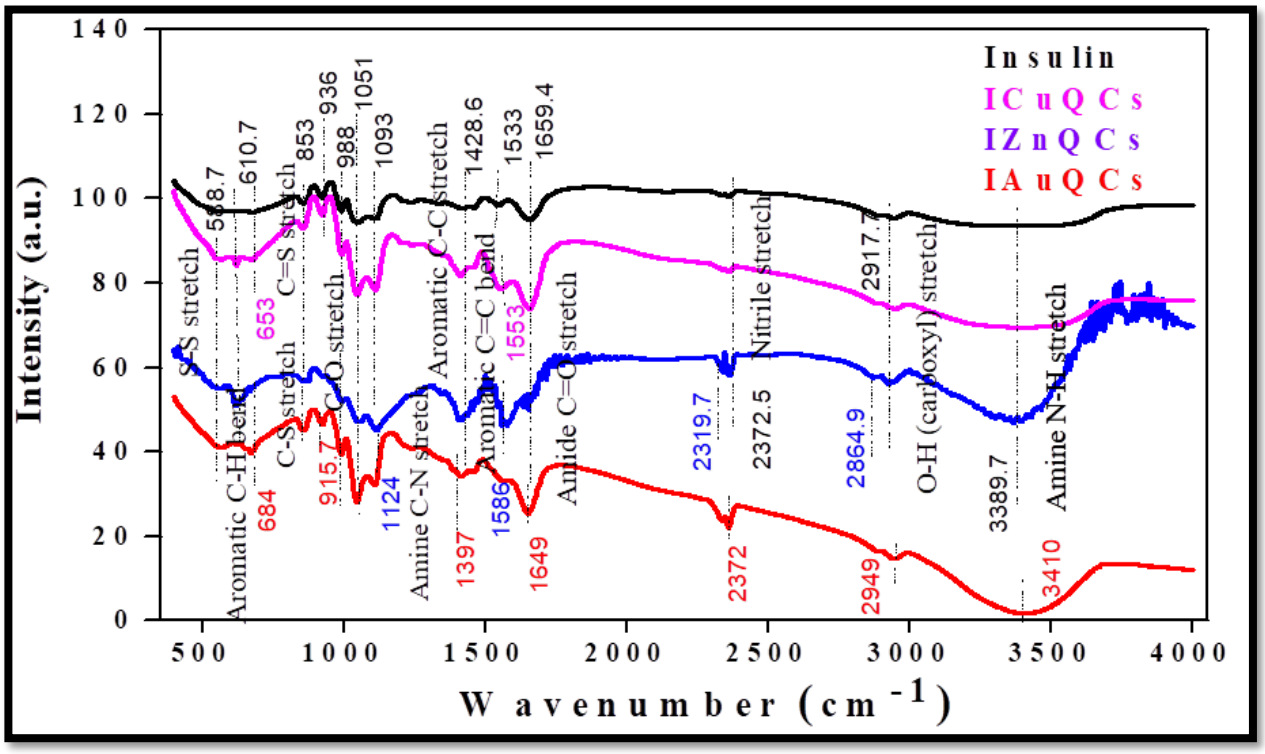

Fig 6: FTIR data of Insulin in comparison with IMQCs where (M= Au, Cu, and Zn).

Functional Groups	Insulin	$CuSO_4$- Insulin	$ZnSO_4$ - insulin	$AuCl_4$ - insulin
S-S stretch	588.7	588.7	588.7	588.7
Aromatic C-H bend	610.7	610.7	610.7	-
C-S stretch	653	653	684	684
C=S stretch	853	853	853	853
C-O stretch	936 988	936 988	- 988	915.7 -
S=O stretch	1051	1051	1051	1051
Amine C-N stretch	1093	1093	1093	1124
Aromatic C-C stretch	1428.6 -	1428.6 -	1428.6 -	1428.6 1397
Aromatic C=C bend	1533	1553	1586	-
Amide C=O stretch	1659.4	1659.4	1659.4	1649
Nitrile stretch	2372.5	2372.5	2372.5 2319.7	2372
O-H stretch	2917.7 -	2917.7 -	2917.7 2864.9	2949 -
Amine N-H stretch	3389.7	3389.7	3389.7	3410

Table 4: Displays the FTIR data of the MQCs Linked with insulin in comparison to each other and insulin.

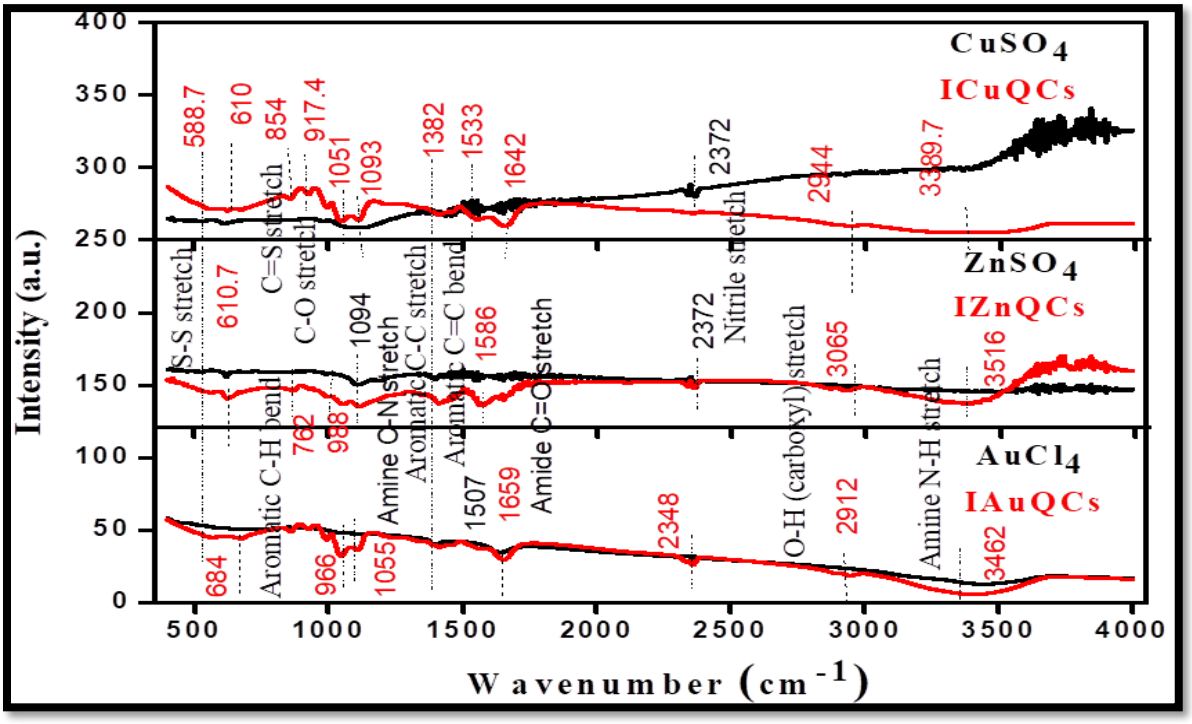

Fig 7 : FTIR data of metal salt solutions in comaprison with their corresponding IMQCs.

Functional Group	$CuSO_4$	$CuSO_4$-Insulin	$ZnSO_4$	$ZnSO_4$-Insulin	$AuCl_4$	$AuCl_4$-Insulin
S-S Stretch	-	588.7	-	588.7	-	588.7
Aromatic C-H bend	-	610	-	610.7	-	684
C=S Stretch	-	854	-	762	-	861.7
C-O stretch	-	917.4	-	988	-	966
S=O stretch	1051	1051	1051	1051	-	1051
Amine C-N stretch	-	1093	-	1094	-	1055
Aromatic C-C stretch	-	1382	-	1382	-	1382
Aromatic C=C bend	-	1533	-	1586	-	1659
Amide C=O stretch	-	1642	-	1642	-	1689
Nitrile stretch	-	2372	-	2372	-	2348
O-H stretch	-	2944 Broad band	-	3065	-	2912
Amine N-H stretch	-	3389.7	-	3516	-	3462

Table 5: Showcases the FTIR data of metal salt solutions in comparison with IMQCs.

4.4 Fluorescence spectrophotometer

The metal salt solutions, the metal salt linked with insulin with and without incubation, and only insulin solution were characterized for analyzing the fluorescence of samples at two excitation wavelengths 302, 365nm.

Insulin shows the emission spectra ranging from 345-500nm upon excitation of 302nm.

IAuQCs at excitation wavelength 302nm shows an emission peak at 399.4 with intensity of 964.3 nm, iAuQCs showed an excitation peak at 397.4nm with intensity at 614.4, for $AuCl_4$ solution the emission peak appeared at 370.3nm with an intensity of 120, only insulin solution showed a peak at only insulin displayed a peak at 440.8nm with intensity of 195.3.

IAuQCs at excitation wavelength 365nm shows an emission peak at 420.7nm with intensity of 137.62, iAuQCs showed an excitation peak at 420.8nm with intensity at 102.7, for AuCl4 solution the emission peak appeared at 415.8nm with an intensity of 62.9, only insulin n xhibited a peak at only insulin showed a peak at 553nm with intensity of 49.76.

ICuQCs at excitation wavelength 302nm shows an emission peak at 400.23nm with intensity of 733.8, iCuQCs showed an excitation peak at 384.4nm with intensity at 537, for $CuSO_4$ solution the emission peak appeared at 387.5nm with an intensity of 205.16; only insulin displayed a peak at only insulin showed a peak at 440.8nm with intensity of 195.3nm

ICuQCs at excitation wavelength 365nm shows an emission peak at 413.2nm with intensity of 255.3, iCuQCs showed an excitation peak at 413.2nm with intensity at 116.2, for $CuSO_4$ solution the emission peak appeared at 413.2nm with an intensity of 81.7, only insulin presented a peak at only insulin showed a peak at 553nm with intensity of nm 49.76.

IZnQCs at excitation wavelength 302nm shows an emission peak at 389.2nm with intensity of 636.37, iZnQCs showed an excitation peak at 393.6nm with intensity at 564.93, for ZnSO4 solution the emission peak appeared at 338.4 nm with an intensity of 72.09, only insulin solution showed a peak at only insulin shoed a peak at 440.8nm with intensity of 195.3nm

IZnQCs at excitation wavelength 365nm shows an emission peak at 416.57 nm with intensity of 329.0, iZnQCs showed an excitation peak at 420nm with intensity at 181.54, for ZnSO4 solution the emission peak appeared at 415.4nm with an intensity of 42.5, only insulin showed a peak at only insulin solution showed a peak at 553nm with intensity of nm 49.76.

For all the three metal salts it has been observed that as we add insulin to the salt solution, the intensity increases. Also it is evident from the table that the incubated sample of the metal salt solutions linked with insulin has much higher intensity than non- incubated sample. Thus the incubated samples exhibit higher fluorescence than non-incubated samples, their corresponding salt solutions and insulin solution.

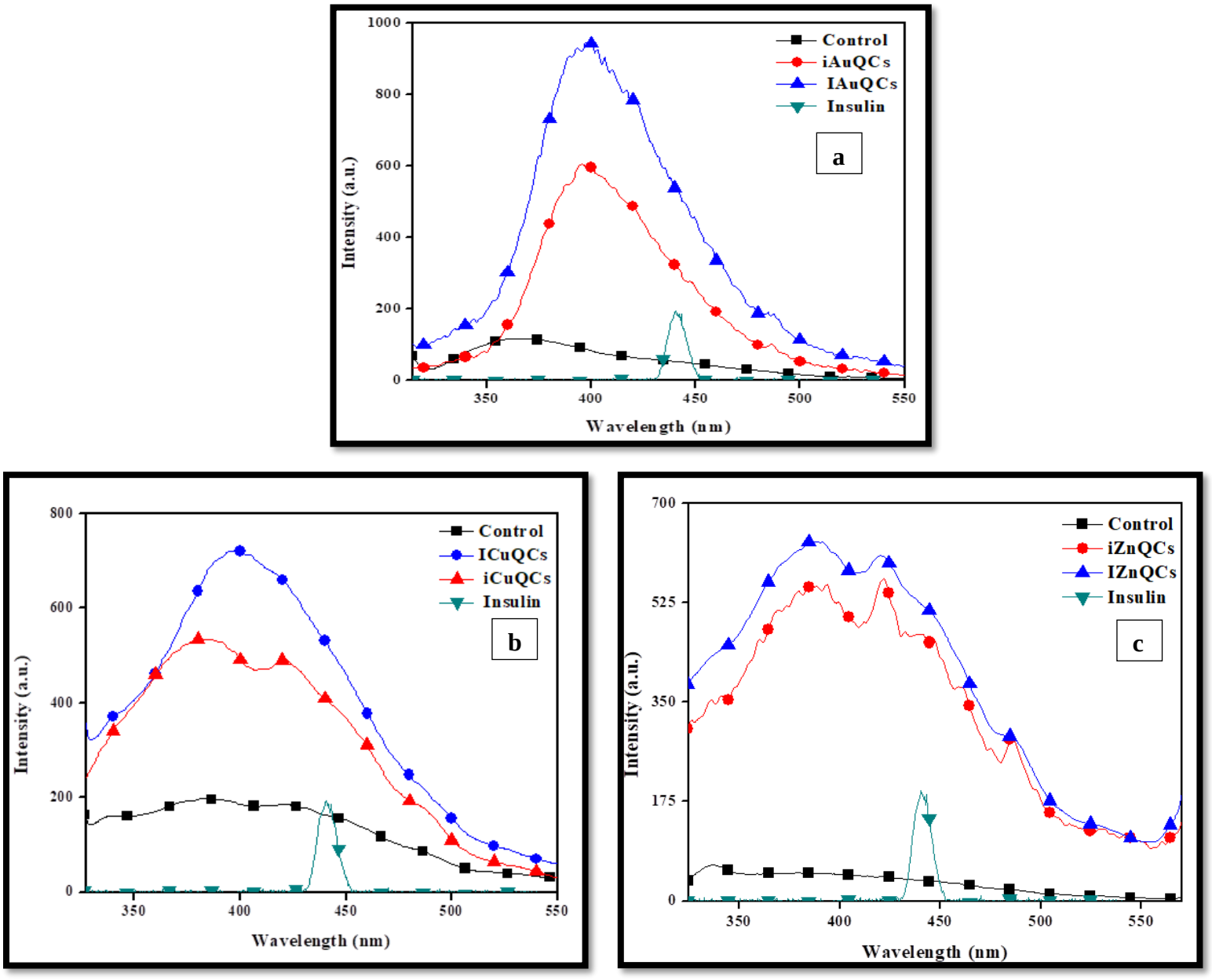

Fig 8: The fluorescence intensity peaks at excitation wavelength of 302nm of IMQCs, iMQCs, insulin solution and metal salt solutions. (M =Au (a), Cu (b), and Zn(c))

Samples at 302nm	Intensity peak	Fluorescence
$AuCl_4$ solution	120	No fluorescence
iAuQCs	614.4	Shows red fluorescence of lower intensity
IAuQCs	964.3	Shows red fluorescence
$CuSO_4$ solution	205	No
iCuQCs	537	Shows blue fluorescence of lower intensity
ICuQCs	733.8	Shows blue fluorescence
$ZnSO_4$ solution	72.09	No
iZnQCs	564.93	Shows green and blue fluorescence of lower intensity
IZnQCs	636.37	Shows green and blue fluorescence
Insulin	195.3	No fluorescence

Table 6: shows the peak intensities of samples at excitation wavelength of 302nm.

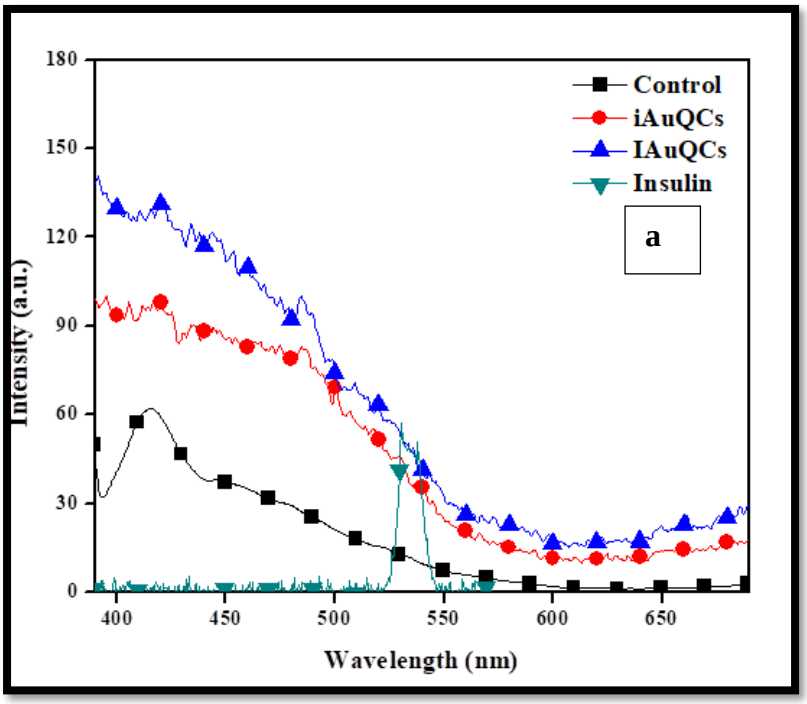

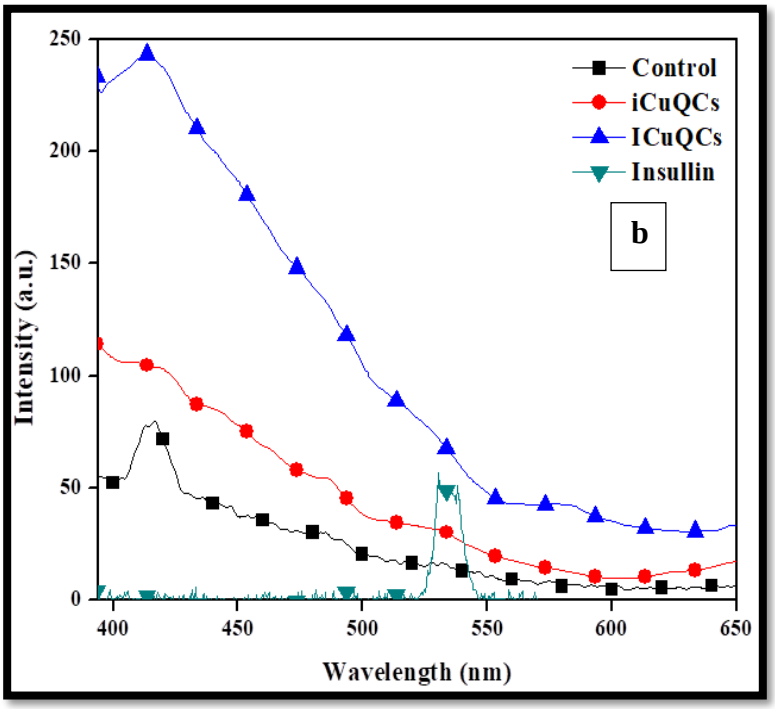

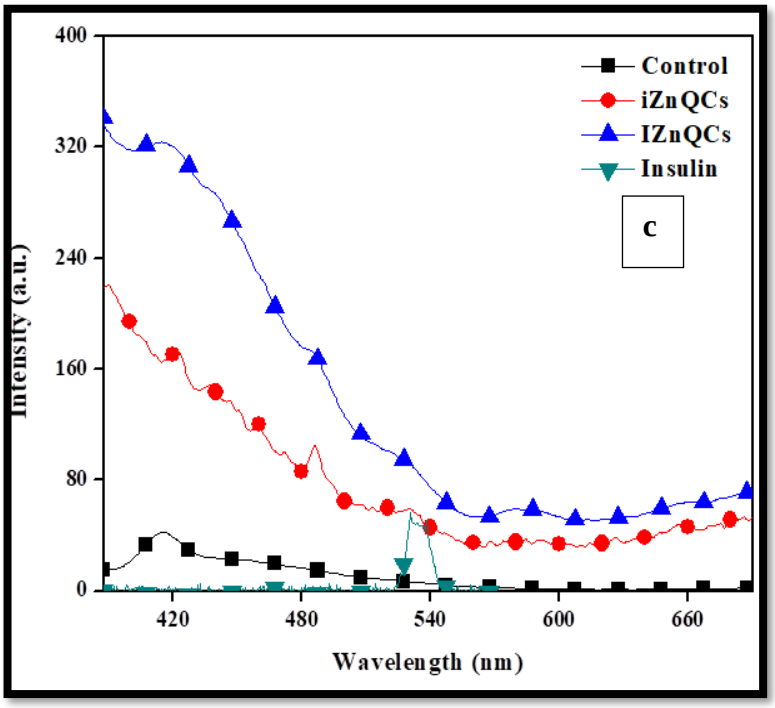

Fi 9: Shows the fluorescence intensity at excitation wavelength 365nm of iMQCs, IMQCs, insulin solution as well as metal salt solutions. (M= Au (a), Cu(b), and Zn(c))

Samples at 365nm	Peak intensity	Fluorescence
$AuCl_4$ Solution	62.9	No
iAuQCs	102.7	Red fluorescence of lower intensity
IAuQCs	137.62	Red fluorescence with higher intensity
$CuSO_4$ solution	81.7	No
iCuQCs	116.2	Blue fluorescence with lower intensity
ICuQCs	255.3	Blue fluorescence with higher intensity
$ZnSO_4$ solution	42.5	No
iZnQCs	181.54	green, blue fluorescence With lower intensity
IZnQCs	329	green ,blue fluorescence with higher intensity
Only insulin	49.76	No

Table 7: Shows intensity peak of samples at excitation wavelength of 365nm.

However, these QCs have prompted excellent fluorescence results for in vivo use. In addition, their larger dimensions, typically comparable to or larger than the size of proteins (like insulin in this case), could possibly alter the purpose of involved ligand molecule [3]. Fluorescent metal NCs are smaller and exhibit bright emission and good biocompatibility, making them attractive alternatives as fluoresent probes for bio-imaging. Hence this was confirmed by performing bio-imaging on A549 cells using fluorescense microscope.

4.5 Fluorescence images

The fluorescence images as mentioned below demonstrated the strong photoluminescence that was displayed by the IMQCs once they were added to the A549 lung cancer cell line. The IMQCs were incubated in UV laminar air flow for 1hr and later they were added to the A549 cancer cell line. Post 2hrs the fluorescence images were observed under the fluorescence microscope.

IAuMQCs showed blue fluorescence that was radiated as a result of binding of the IAuMQCs with the insulin receptors present on the surface of the A549 lung cancer cell lines **(Fig 10).**

The same phenomena was observed in ICuMQCs **(Fig 11)** that display blue fluorescence, IZnMQCs on the other hand shows dual fluorescence of **(Fig 12, 13)** blue and green fluorescence respectively. Owing to the binding of the samples with the surface insulin receptors.

These images are symmetrical with the fluorescence emission peaks that were analyzed via fluorescence spectroscopy.

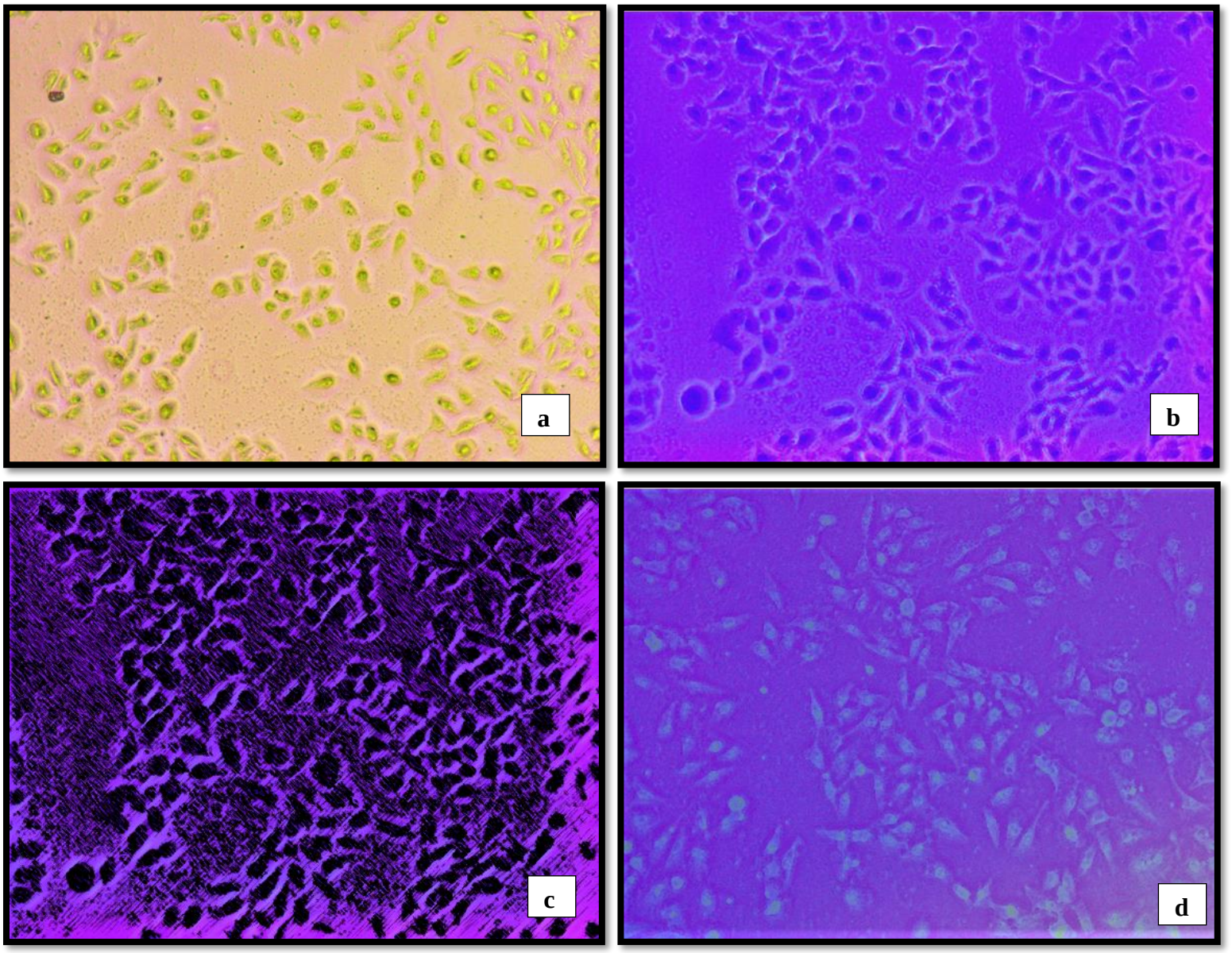

Fig 10 : (a) Shows the the cells treated with the sample(IAuQCs) in visible light (b)it shows the blue fluorescence image of the cytosolic membrane. (c) Software edited image which enhances the fluorescence radiated by the cytosoloic membrane. (d) It shows the blue fluorescence of the IAuQCs on the cell surface.

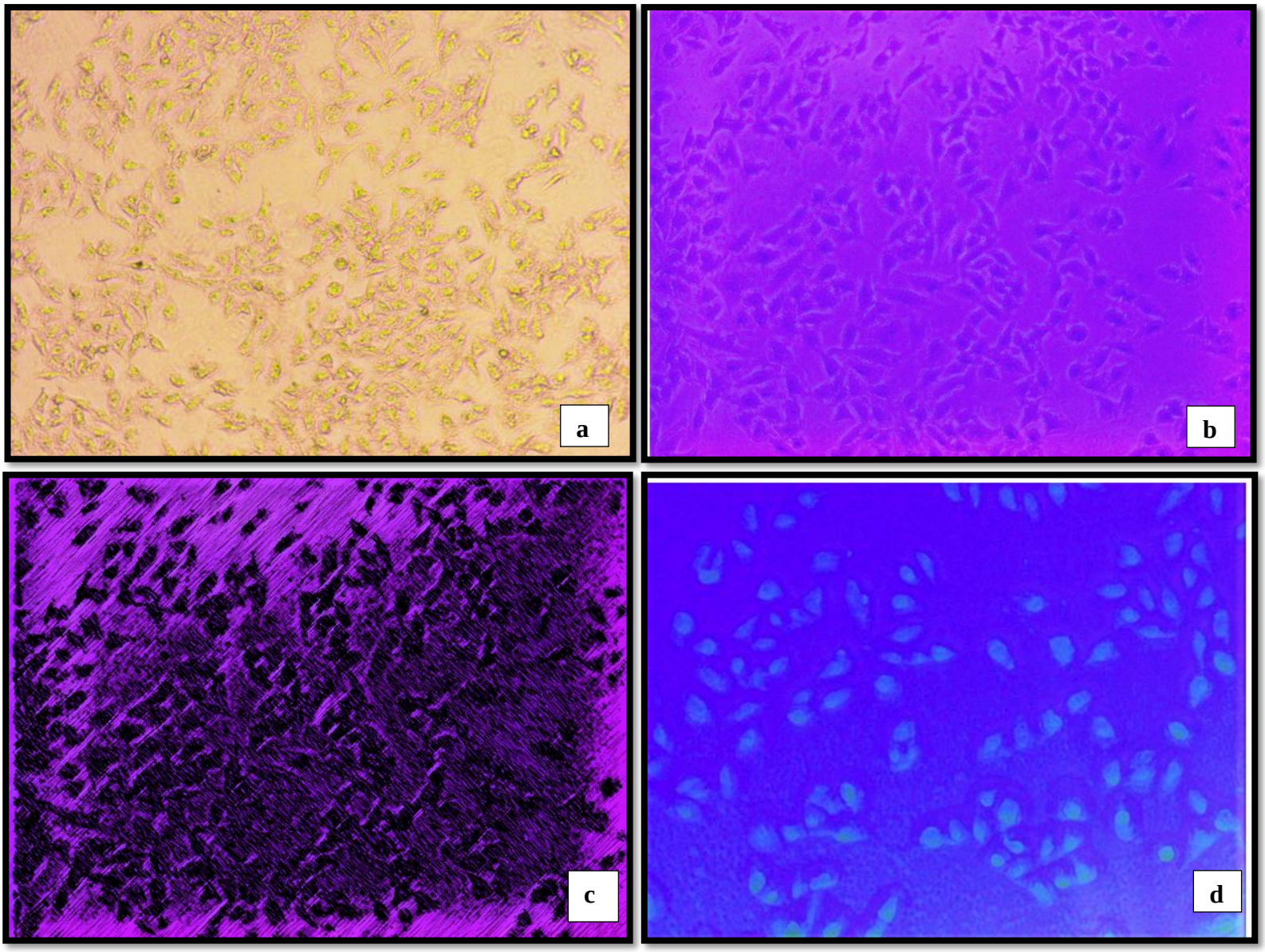

Fig 11: (a) Shows the cells treated with sample (ICuQCs) in visible light. (b) It shows the blue fluorescence radiated by the cytosolic membrane. (c) Software edited image of the same sample which enhance sthe fluorescence radiated by cytosolic membrane. (d) This image shows the fluorescence emitted by the cell surface.

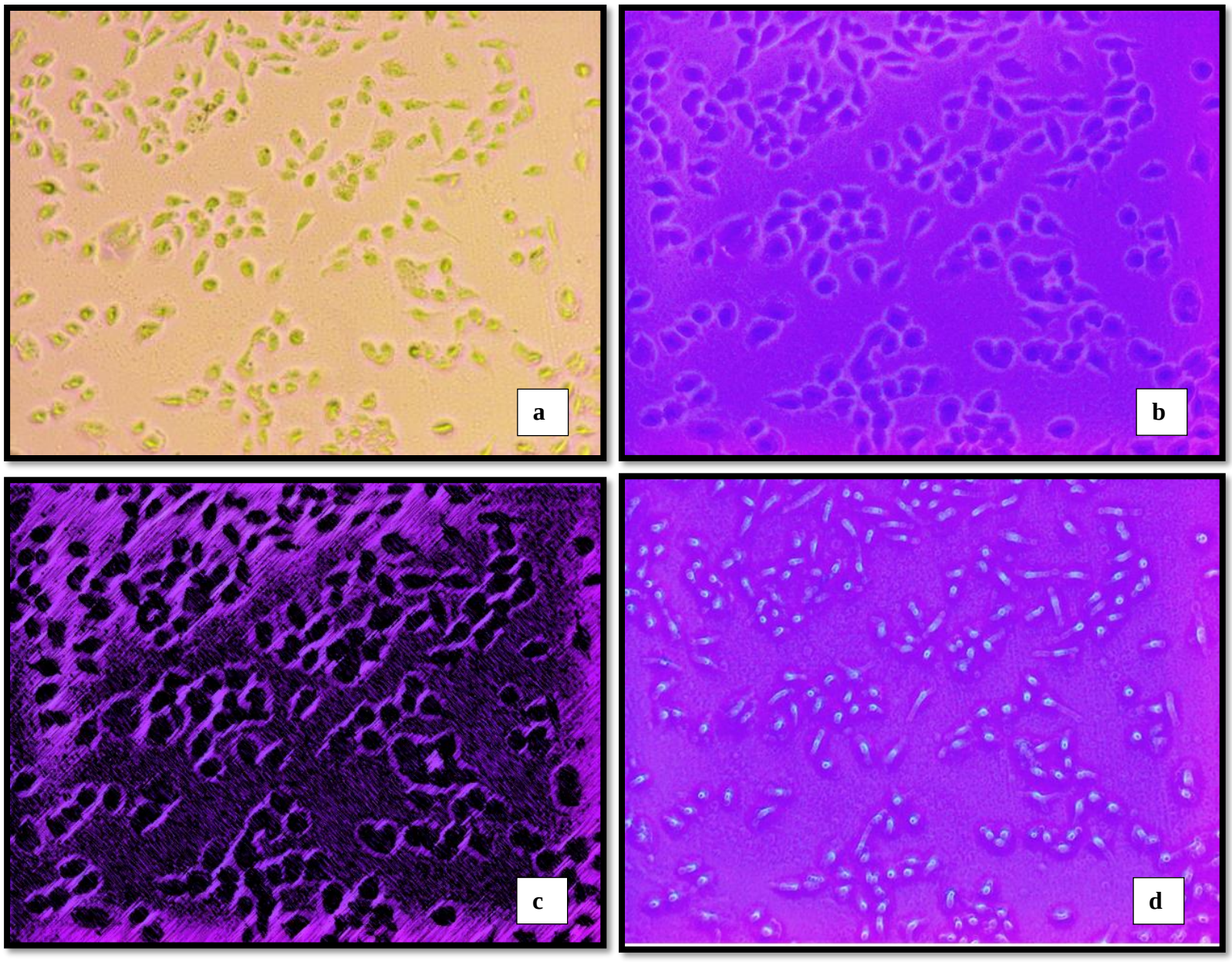

Fig 12 : (a) Respresents image of the cells treated with IZnQCs in visible light.

(b) Displays the image of cells treated with IZnQCs showcasing blue fluorescence. (c) Software edited image of the cells treated with IZnQCs to enhance blue fluorescence. (d) this image depicts blue fluorescence radiated by the cells.

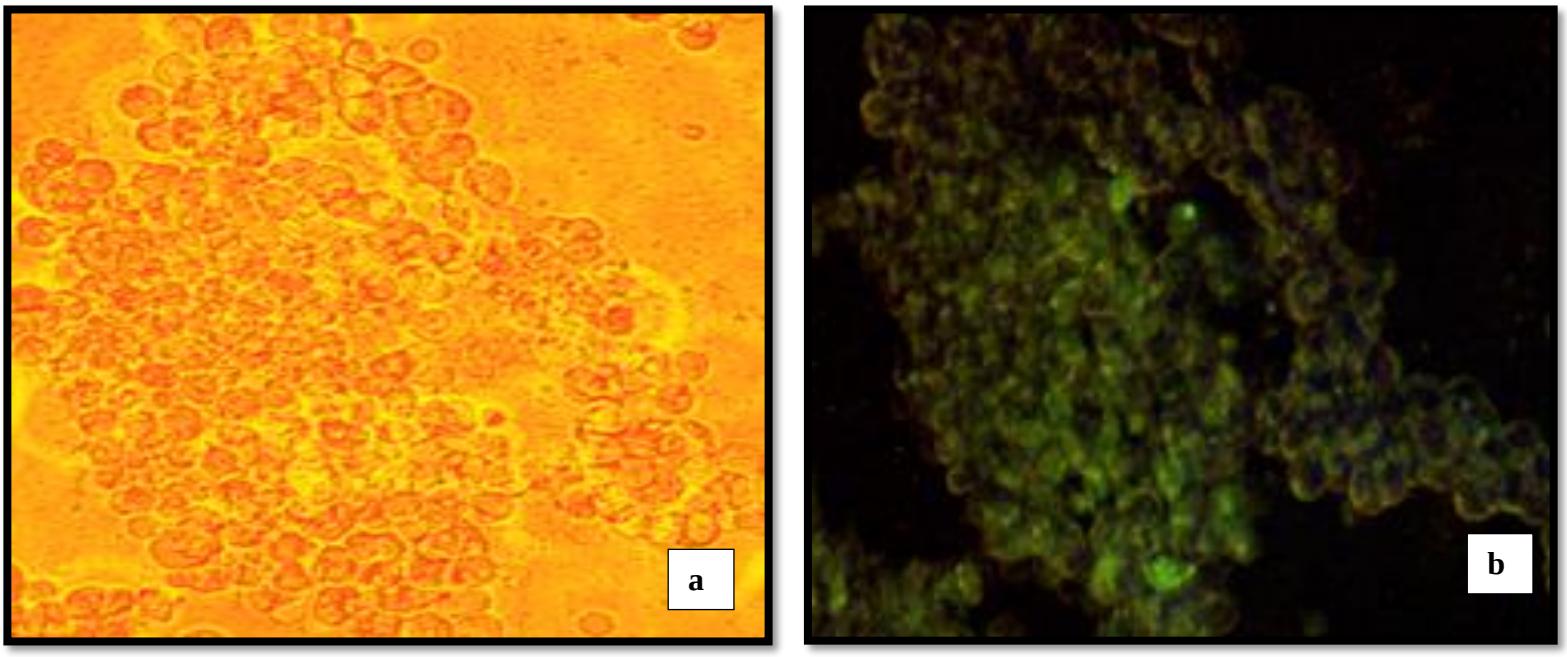

Fig 13 : (a) it shows the image of the cells treated with IZnQCs in visible light. (b) it shows the image of the the cells tretaed with IZnQCs, displaying green fluorescence.

4.5 SEM-EDS

SEM/EDS analysis was supported out in a high vacuum using a JEOL JSM 6490LV scanning electron microscope (SEM) coupled with an Oxford INCA energy dispersive spectroscopy (EDS) system. The EDS microanalysis relies upon a few variable components, for example, the quantity of identified X-beams produced from constituent components in the sample under investigation and impacts of spectral interference as well as background disturbances. These features may vary from analysis to analysis. Accuracy coupled with precision was resolved all together to evaluate repeatability of estimations. We determined the chemical composition of the IMQCs (where M = Au, Cu, and Zn) using SEM/EDS. A typical spectrum where separate peaks of Au and S (from insulin) were used to determine relative atomic concentrations. The presence of Au along with other elements like C,Cl,S,P,Na,O were detected (as shown in **Table 8**), the elements present in Cu and Zn are also shown in **Table 8** and **table 9** respectively . The ratio of Au to S (cysteine molecules in) is approximately (1.56) 2. Which suggests that 2 atoms of Au are inserted in 2 molecule if insulin. The ratio of Au to S (cysteine molecules in) is approximately (1.56) 2. The ratio of Cu to S is approximately (1.95) 2. Which suggests that 2 atoms of Cu are inserted in 2 molecule if insulin. Similarly for Zn, the ratio of Zn to S is 0.078.

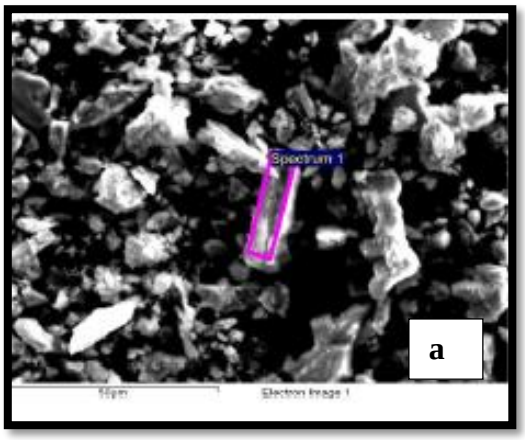

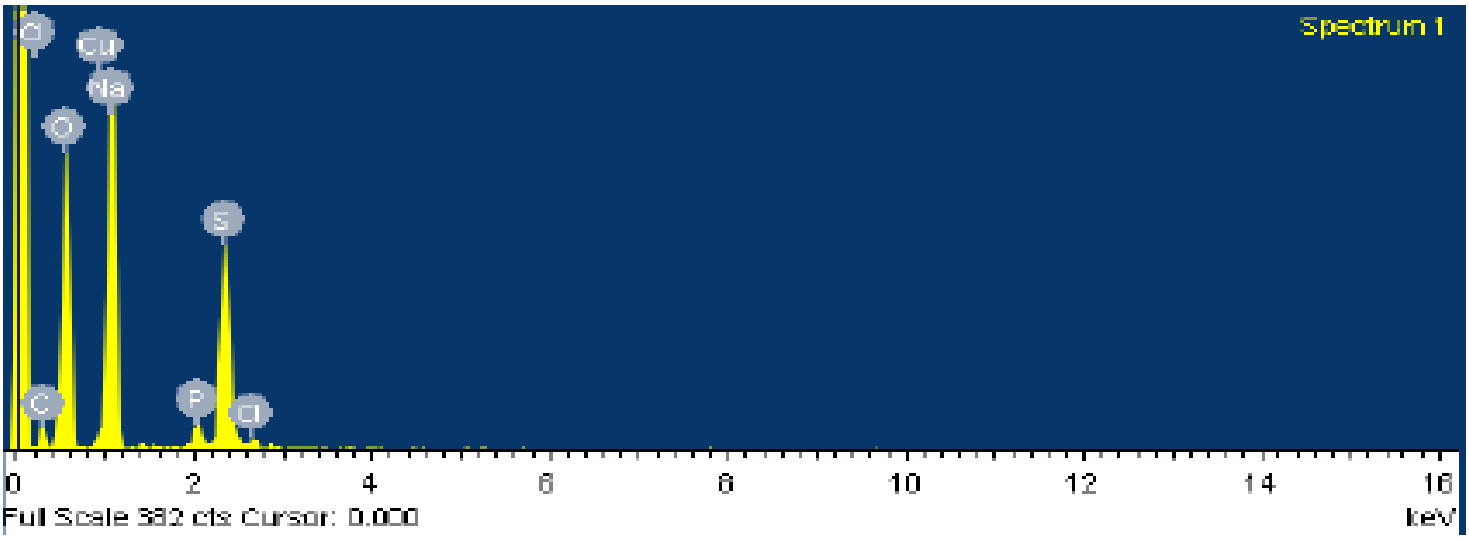

Fig 14: (a) It represents SEM image of ICuQCs. (b) EDS spectrum of ICuQCs depicting elemental composition of the sample.

ELEMENTS	ATOMIC (%)
C	22.59
O	40.28
Na	19.53
P	1.346
S	17.48
Cl	1.896
Cu	3.84

Table 8: It shows the fundamental composition (in atomic %) of the ICuQCs.

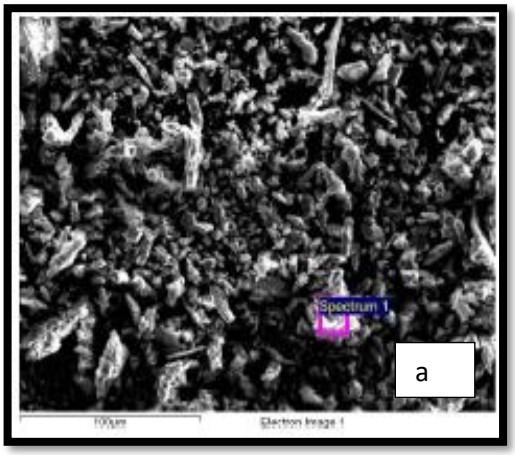

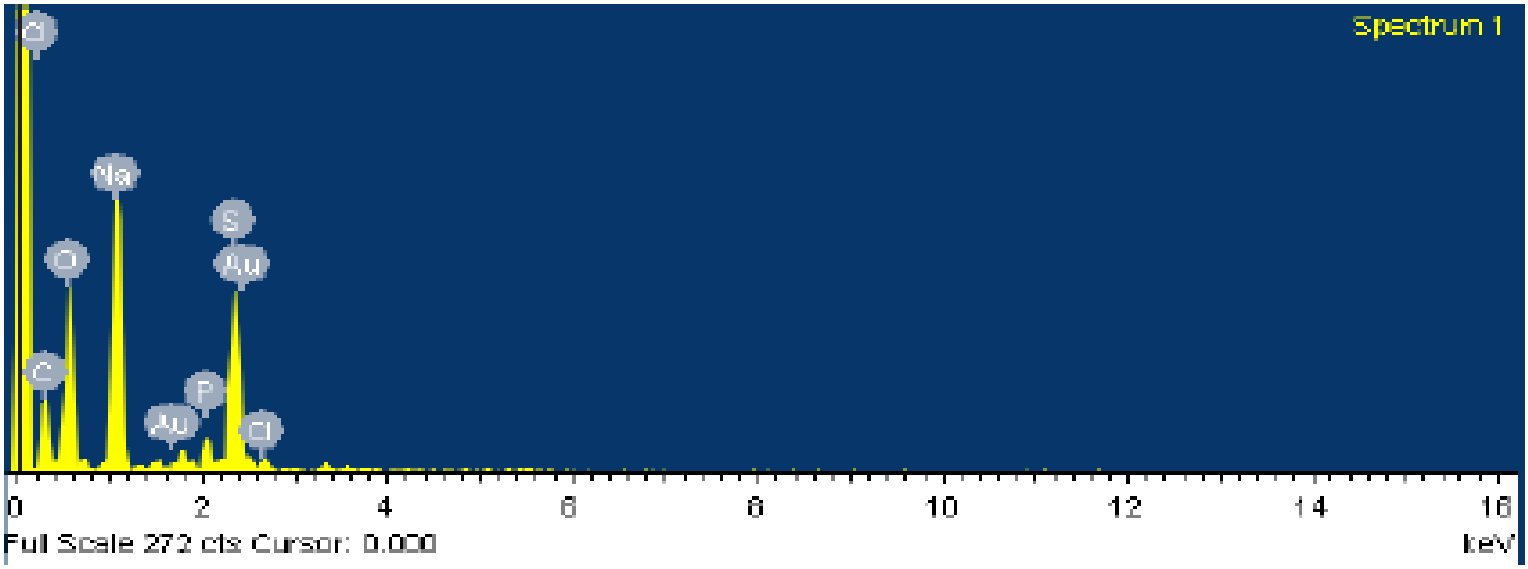

Fig 15: (a) It represents the SEM image of IAuQCs. (b) The EDS spectrum of the IAuQCs depicting elemental composition.

ELEMENTS	ATOMIC (%)
C	34
O	33.8
Na	14.49
P	1.93
S	10.94
Cl	2.32
Au	2.86

Table 9: It shows the fundamental composition (in atomic %) of the sample IAuQCs.

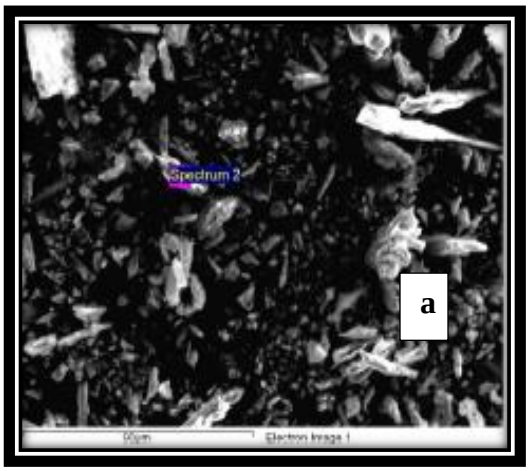

Fig 16: (a) It represents the SEM image of IZnQCs. (b) The EDS spectrum of the IZnQCs, depicting elemental composition.

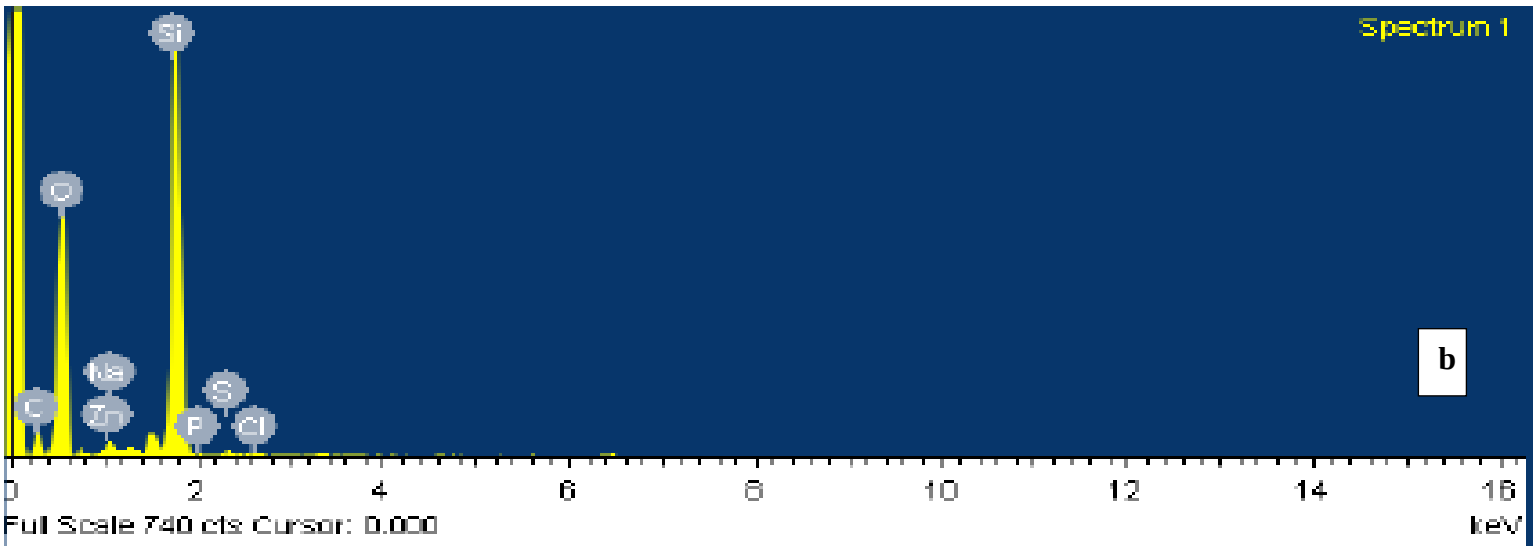

ELEMENTS	ATOMIC (%)
C	26.31
O	52.43
Na	20.46
P	5.69
S	12.15

Cl	**1.34**
Zn	**0.158**

Table 10: It shows the fundamental composition (in atomic %) of the sample IZnQCs.

4.6 Conclusion and Future perspective

In conclusion water soluble metal linked Insulin quantum clusters were synthesized successfully via NaOH mediated synthesis.

In this thesis an interdisciplinary system of biology and chemical sciences has been demonstrated. Metal quantum clusters offer variety of advantages like low toxicity, high photoluminescence, higher photostability, and enhanced biocompatibility. All of these advantages coupled with the fascinating benefit of being coupled in a bio-molecular matrix.

Facile synthesis procedure was opted for the preparation of water soluble bio-functionalized protein scaffold protected metal quantum clusters.

The UV and DLS results confirmed the formation of spherical clusters of IMQCs and size of the IMQCs respectively. The FTIR data was analyzed to confirm the formation of insulin linked IMQCs with the detection of functional groups which were found to be similar in Insulin and IMQCs. The IMQCs exhibited luminescence which was confirmed by fluorescence spectrophotometer. The graphs were analyzed at excitation wavelengths of 302nm and 365nm. IAuQCs and ICuQCs demonstrated blue fluorescence while IZnQCs exhibited dual fluorescence of blue and green. This result was in symmetry with fluorescence images obtained after treating these clusters with A549 lung cancer cell line.

SEM/EDS analysis gave the result of the elemental composition (% by weight) ratio of the S (from cysteine present in insulin) to the amount of Au, Cu and Zn present in the sample.

The comprehensive understanding of the structures and properties of metal quantum-clusters is still in its infant stage. The stability of metal quantum clusters in-vivo is still a challenging issue. Molecular mechanisms and dynamics based computational programs will help refine the research progress. For deeper understanding, crystal structures of the metal embedded in the protein matrix is highly important. The fluorescent metal quantum clusters capped with protein can be utilized as catalysts by exploiting the functionality of the protein. One of the most basic aspects that have to be taken care of is that what will be the fate of these metal lined protein quantum clusters once they enter the biological system. We can utilize it to grow virus linked quantum clusters.

Chapter 5

References

(1) Pyng Y.; Xiaoming W.; Yon-Rui T.; Xiaoqian M.; and Jau T.; Part. Part. Syst.Charact. **2014.**

(2) Yuan, X.; Luo, Z.; Zhang, Q.; Zhang, X.; Zheng, Y.; Lee, J.; Xie, J. ACS Nano (5), 8800-8808, **2011.**

(3) Shang, L.; Dong, S.; Nienhaus, G. Nano Today (6), 401-418, **2011.**

(4) Weibin Z and Franc-ois B., American chemical society (5),10,8013–8018, **2011.**

(5) Xavier, P.; Chaudhari, K.; Baksi, A.; Pradeep, T. Nano Reviews, (3), 14767, **2012.**

(6) Shang, L.; Dong, S. Chemical Communications 1088, **2008.**

(7) Shang, L.; Dong, S.; Nienhaus, G. Nano Today, (6), 401-418, **2011**.

(8) Paulrajpillai L.X.; Kamalesh C.; Pramod K.V.; Samir K.P.; and Thalappil P.; Nanoscale, (2), 2769–2776, **2010.**

(9) T.U.B.Rao and Pradeep T.; Angew. Chem Int. Ed.; (49), 3925–3929, **2010**.

(10) Shang, L.; Dong, S.; Nienhaus, G. Nano Today, (6), 401-418, **2011.**

(11) nanobiotechnology (accessed Jun 28) **2018**.

(12) Samori, B.; Angewandte Chemie , 120, 242-243, **2008.**

(13) Rao J.; Dragulescu-Andrasi A.; Yao H.; Current Opinion in Biotechnology (18), 17-25, **2007.**

(14) Hua He.; Chao Xie.; Jicun Ren.; Anal.Chem. **(**80), 5951–5957, **2008.**

(15) Jianghong R.; Anca D.A.; and Hequan Y.; Science direct, (18), 17–25, **2007.**

(16) Koutecky J.; Fantucci P.; Chemical Reviews, (86), 539-587, **1986.**

(17) Muthaiah S.; and Kien W S.; Chemosensors ,(5), 36, **2017.**

(18) Cheng-An J.L.; Chih-Hsien L.; Jyun-Tai H.; Hsueh-Hsiao W.; Jimmy K.L.; Ji-Lin S.; Wen-Hsiung C.; Hung Y.; Walter H. C.; J. Med. Biol. Eng., (6) ,29, **2009.**

(19) Khandelwal, P.; Poddar, P. Journal of Materials Chemistry B, (5), 9055-9084, **2017.**

(20) Li Shang.; and G. Ulrich Nienhaus.; APL Materials (**5)**, 053101, **2017.**

(21) Tan X.; Jin R. Wiley.; (5), 569-581, **2013**.

(22) Lebedev V.S.; Medvedev A.S.; Vasil'ev D.N.; Chubich D.A.; Vitukhnovsky A.G.; Quantum Electronics 40 (3) 246 -253, **2010.**

(23) Tingting Z.; Tingyao Z.; Qiuhong Y.; Chunli H.; and Xi C.; China Journal of Environmental Science and Health, 168-187, **2015.**

(24) Nirmal G.; Qiaofeng Y.; Zhentao L.; Jingguo L.; Tiankai C.; and Jianping Xie J.; Phys. Chem. Lett.; (7), 962−975, **2016.**

(25) Jain P. K.; Huang X.; El-Sayed I. H.; El-Sayed M.A.; Acc. Chem. Res. (41), 1578−1586, **2008.**

(26) Pdbe.org

(27) peking insulin structure research group Sci. Sin.(17) 752-778, **1974.**

(28) Insulin research group Academia sinica ibid. P (17) 779-792, **1974.**

(29) Sara sleigh Journal of Diabetes Nursing (5), 132 – 158, **1998.**

(30) Adams M.J.; Blundell T.L.; Dodson E.J.; et al Nature, (5), 491, **1969.**

(31) Muhammed M. A. H..; Verma P. K. .; Pal S. K., Arun Kumar R. C.; Paul S.; Omkumar R. V.; and Pradeep T.; Chem.–Eur. J., (15) ,10110–10120, **2009.**

(32) Chen W.Y.; Huang C.C.; Chen L.Y.; Chang H.T, Nanoscale (6),11078−11083, **2014.**

(33) Wilcoxon, J.; Abrams, B. Chemical Society Reviews, (35), 1162, **2006.**

(34) Yuan, X.; Luo, Z.; Zhang, Q.; Zhang, X.; Zheng, Y.; Lee, J.; Xie, J. ACS Nano, (5), 8800-8808, **2011.**

(35) Li M.; Yang D.; Wang X.; Lu J.; Cui D. Nanoscale Research Letters, (8), 182, **2013**.

(36) Xiaohong T.; and Rongchao J.; WIREs Nanomed Nanobiotechnol**, 2013.**

(37) Yu J.; Choi S.; Richards C.I.; Antoku Y.; Dickson R.M.; Photochem Photobiol *(*84), 1435–1439, **2008.**

(38) Liu C.L.; Wu H.T.; Hsiao Y.H.; Lai C.W.; Shih C.W.; Peng Y.K.; Tang K.C.; Chang H.W.; Chien Y.C.; Hsiao J.K.; Angew Chem Int Ed,(50),7056–7060, **2011.**

(39) Rao J.; Dragulescu-Andrasi A.; Yao H.; Curr Opin Biotechnol, (18),17–25, **2007.**

(40)Yang L.; Shang L.; Nienhaus GU.; Nanoscale, (5),1537–1543, **2013.**

(41) Yu Tao.; Mingqiang L.; Jinsong Rena.; and Xiaogang Qu.; Chem. Soc. Rev**,** (44), 8636, **2015.**

(42) X. Ji.; F. Peng.; Y. Zhong.; Y. Su.; X. Jiang.; C. Song.; L. Yang.; B. Chu.; S.-T. Lee.; and Y. He.; Adv. Mater, (27), 1029, **2015.**

(43) H. Wei , Z. Wang , L. Yang , S. Tian , C. Hou , Y. Lu , Analyst (135) ,1406, **2010**.

(44) L. Hu.; S. Han.; S. Parveen.; Y. Yuan.; L. Zhang.; G. Xu.; Biosens. Bioelectron. (32) , 97,**2011**.

(45) Xie J.;Zheng Y.; Ying JY.; Chem Commun,; (46), 961, **2010.**

(46) Goswami N.; Giri A.; Bootharaju MS.; Xavier P.L.; Pradeep T.; Pal S.K.; Anal Chem, (24), 9676, **2011.**

(47). Li L.; Liu H.; Shen Y.; Zhang J.; Zhu JJ.; Anal Chem; (8),661, 2011.

(48). Fang Y.M.; Song J.; Li J.; Wang Y.W.; Yang H.H.; Sun J.J.; Chem Commun (47), 2369, **2011.**

(49). Chen Y.; Shen Y.; Sun D.; Zhang H.; Tian D.; Zhang J.; Chem Commun; (47), 11733, **2011.**

(50). Retnakumari A.; Jayasimhan J.; Chandran P.; Menon D.; Nair S,; Mony U.; nanotechnology, (22), 285102,**2011.**

(51). Wang Y.; Chen J.; Irudayaraj J.; ACS Nano (12), 9718, **2011**.

(52). Durgadas CV.; Sharma CP.; Sreenivasan K.; Analyst,; (136), 933, **2011.**

(53). Durgadas CV,; Sharma CP,; Sreenivasan K.; Nanoscale, (11) 4780, **2011.**

Sherya thesis

ORIGINALITY REPORT

3%	1%	2%	%
SIMILARITY INDEX	INTERNET SOURCES	PUBLICATIONS	STUDENT PAPERS

PRIMARY SOURCES

1	www.nano-reviews.net Internet Source	1%
2	Tao, Yu, Mingqiang Li, Jinsong Ren, and Xiaogang Qu. "Metal nanoclusters: novel probes for diagnostic and therapeutic applications", Chemical Society Reviews, 2015. Publication	1%
3	Tan, Xiaohong, and Rongchao Jin. "Ultrasmall metal nanoclusters for bio-related applications : Ultrasmall metal nanoclusters", Wiley Interdisciplinary Reviews Nanomedicine and Nanobiotechnology, 2013. Publication	1%
4	Innocent B. Bekard, Dave E. Dunstan. "Tyrosine Autofluorescence as a Measure of Bovine Insulin Fibrillation", Biophysical Journal, 2009 Publication	<1%
5	Yu, Pyng, Xiaoming Wen, Yon-Rui Toh, Xiaoqian Ma, and Jau Tang. "Fluorescent Metallic Nanoclusters: Electron Dynamics,	<1%

Sherya.

Structure, and Applications", Particle & Particle Systems Characterization, 2014.
Publication

6 Xun Yuan, Zhentao Luo, Qingbo Zhang, Xinhai Zhang, Yuangang Zheng, Jim Yang Lee, Jianping Xie. "Synthesis of Highly Fluorescent Metal (Ag, Au, Pt, and Cu) Nanoclusters by Electrostatically Induced Reversible Phase Transfer", ACS Nano, 2011 <1%
Publication

Exclude quotes	On	Exclude matches	< 10 words
Exclude bibliography	On		